SynOpen

Recent catalytic applications of porphyrin and phthalocyanine-based nanomaterials in organic transformations

Raveena Raveena, Anju Bajaj, Astha Tripathi, Pratibha Kumari.

Affiliations below.

Conflict of Interest:

Abstract:
Catalysis is a great tool for synthesizing many molecular scaffolds for various applications, including fuels, pharmaceuticals, fertilizers, fabrics, and fragrances. Different metal complexes of porphyrin and phthalocyanines have been developed as promising catalysts for various catalytic transformations under mild conditions, which mimic the action of cytochrome P450 enzymes. The efficiency and selectivity of porphyrins and phthalocyanine-based catalysts have been significantly enhanced by making their nanocomposites. Porphyrins and phthalocyanines have been modified by various nanomaterials such as metal nanoparticles, metal oxide nanoparticles, carbon-based nanomaterial, and nano-organic frameworks such as metal-organic frameworks and covalent-organic frameworks. Their photo-physical and catalytic activities have been studied in various organic transformations. The formation of different nanocomposites of porphyrin and phthalocyanines has been summarized, and their chemical, electrochemical, and photo-catalytic applications in different organic transformations as catalysts have been reviewed.

Corresponding Author:
Dr. Pratibha Kumari, Deshbandhu College, University of Delhi, Chemistry, Deshbandhu College, University of Delhi, 110019 Delhi, India, pkumarichemistry@gmail.com

Affiliations:
Raveena Raveena, Deshbandhu College, Chemistry, New Delhi, India
Anju Bajaj, ARSD College, Chemistry, New Delhi, India
Astha Tripathi, Deshbandhu College, Chemistry, New Delhi, India
Pratibha Kumari, Deshbandhu College, University of Delhi, Chemistry, Delhi, India

Accepted Manuscript

Thieme

Recent catalytic applications of porphyrin and phthalocyanine-based nanocomposites in organic transformations
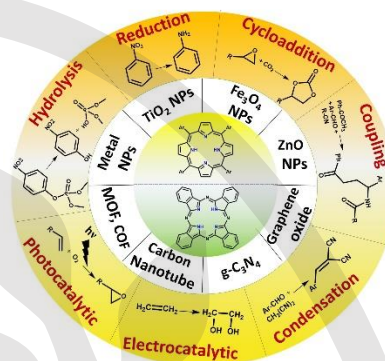
Raveena[a,b]
Anju Bajaj[c]
Astha Tripathi[a,b]
Pratibha Kumari*[,b]

[a]Department of Chemistry, University of Delhi, New Delhi 110007, India

[b]Bioorganic Material Research Laboratory, Department of Chemistry, Deshbandhu College, University of Delhi, Kalkaji New Delhi 110019, India

[c]Department of Chemistry, ARSD College, University of Delhi, New Delhi, India

*Email: pkumarichemistry@gmail.com

Abstract Catalysis is a great tool for synthesizing many molecular scaffolds for various applications, including fuels, pharmaceuticals, fertilizers, fabrics, and fragrances. Different metal complexes of porphyrin and phthalocyanines have been developed as promising catalysts for various catalytic transformations under mild conditions, which mimic the action of cytochrome P450 enzymes. The efficiency and selectivity of porphyrins and phthalocyanine-based catalysts have been significantly enhanced by making their nanocomposites. Porphyrins and phthalocyanines have been modified by various nanomaterials such as metal nanoparticles, metal oxide nanoparticles, carbon-based nanomaterial, and nano-organic frameworks such as metal-organic frameworks and covalent-organic frameworks. Their photo-physical and catalytic activities have been studied in various organic transformations. The formation of different nanocomposites of porphyrin and phthalocyanines has been summarized, and their chemical, electrochemical, and photo-catalytic applications in different organic transformations as catalysts have been reviewed.

1. Introduction
2. Porphyrin and phthalocyanine-based nanocomposites for catalytic applications
2.1 Porphyrin and phthalocyanine-based nanocomposites with metal nanoparticles
2.2 Metal oxide nanoparticles modified porphyrin and phthalocyanine nanocomposites
2.2.1 Nanoconjugates of porphyrin and phthalocyanine with magnetic nanoparticles
2.2.2 Nanocomposites of porphyrin and phthalocyanine with titanium oxide nanoparticles
2.3 Porphyrin and phthalocyanine-based nanocomposites with carbon-based nanomaterial
2.3.1 Porphyrin and phthalocyanine nanocomposites with carbon nanotubes
2.3.2 Porphyrin/phthalocyanine-based nanocomposites with graphene oxide
2.3.3 Porphyrin and phthalocyanine nanocomposites with graphitic carbon nitrite
2.4 Porphyrin and phthalocyanine-based nano-organic framework
3. Conclusion and Future Prospects

1. Introduction

The catalytic application of porphyrin- and phthalocyanine-based nanomaterials for organic transformations has garnered significant attention due to their unique structural, electronic, and chemical properties. Both porphyrins and phthalocyanines are macrocyclic compounds with a conjugated 18 π-electron system and high thermal and chemical stability. Their ability to coordinate with various metal ions and their tunable electronic properties make them highly versatile in catalysis. The central cavity of these macrocycles can host metal ions such as iron, cobalt, manganese, and copper, enhancing their catalytic activity through redox reactions, electron transfer, and activation of substrates. Additionally, their extended conjugated systems enable efficient light absorption, making them suitable for photocatalytic reactions. Their catalytic behavior can be further enhanced by introducing different substituents on the macrocyclic ring, which can affect their solubility, electronic properties, and catalytic behavior. Porphyrin and phthalocyanines are the most utilized catalysts in various organic transformations.[1–6] Figure 1 represents some recently used functionalized porphyrin and phthalocyanine derivatives to catalyze oxidation and addition reactions during 2020-2024 (Table 1).

The formation of nanocomposites of porphyrin and phthalocyanine transforms their catalytic properties by increasing surface area, improving substrate interaction, and enhancing the dispersion of active sites. Nanomaterials used to prepare nanocomposites of these macrocycles include metal nanoparticles, metal oxide nanoparticles, carbon nanostructures, and nano organic-frameworks such as metal-organic frameworks (MOFs) and covalent-organic frameworks (COFs). These advanced materials have demonstrated improved catalytic activity and selectivity compared to their bulk counterparts. Porphyrins and phthalocyanine-based nanomaterials have been employed in a wide range of organic reactions such as oxidation of alcohols, sulfides, and olefins;

reduction of nitro compounds and carbonyl compounds; the C-C and C-N bond forming reactions; and photocatalytic degradation of pollutants and synthetic reactions. Porphyrins and phthalocyanines act as photosensitizers to generate singlet oxygen in the presence of light by the photoinduced energy transfer process. The reactive oxygen species have oxidized many organic compounds. However, these photoactive macrocycles usually counter the issue of deactivation and aggregation of catalysts, limiting their broad applicability. Their hybrids with nanomaterials make them highly stable, along with the availability of more catalytic active sites for the reactions.
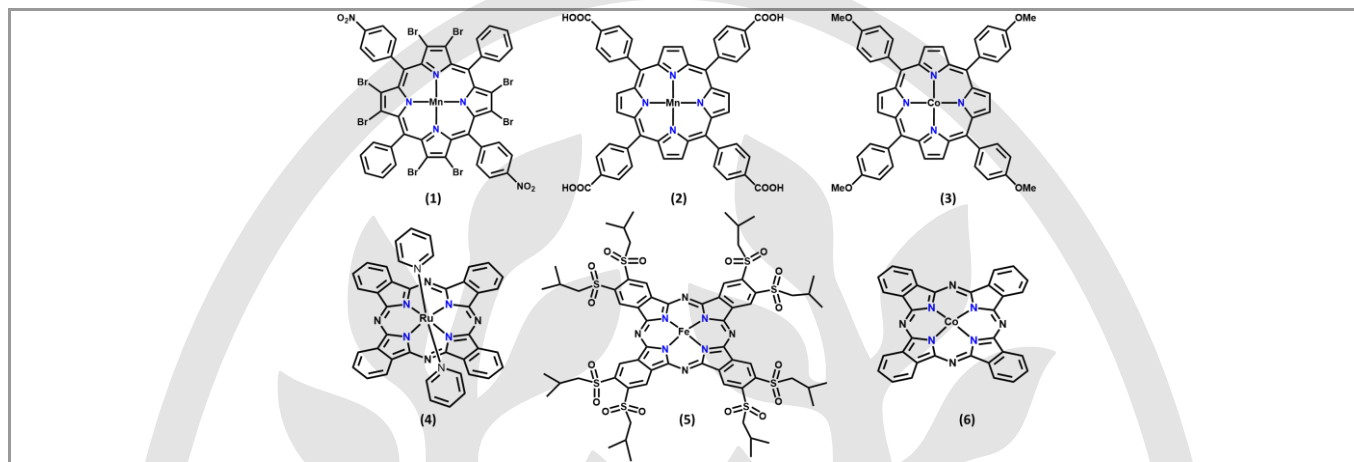

Figure 1 Structure of some recently used porphyrin and phthalocyanine catalysts

Table 1 Some recent reactions catalyzed by porphyrins (**1-3**) and phthalocyanines (**4-6**)

Entry	Catalyst	Reactant	Product (Yield)	Reaction Conditions	Reaction Type	Reference
1	Mn (III) porphyrin (**1**)	cyclohexane	cyclohexanol (56 %), cyclohexanone (24 %)	PhIO, 25 ℃, 90 min.	Oxidation	7
2	Mn (III) porphyrin (**2**)	epoxide + CO_2	cyclic carbonates (99-41 %)	CO_2 (1 atm), TBAI, 90 ℃, 36 h	cycloaddition	8
3	Co (II) porphyrin (**3**)	dibenzothiophene	dibenzothiophene sulphone (95 %)	H_2O_2, CH_3CN, 50 ℃, 45 min.	oxidation	9
4	Ru (II) phthalocyanine (**4**)	alkenes + CF_3SO_2Cl	chlorotrifluoromethyl (94 %)	red LED light, K_2HPO_4, room temperature (RT), 20 h	Trifluoromethylation	10
5	Fe (II) phthalocyanine (**5**)	cyclohexene	2-cyclohexen-1-one (51 %), 2-cyclohexen-1-ol (18 %), cyclohexene oxide (2 %)	TBHP, CH_3CN, 40 °C, 5 h	Oxidation	11
6	Co (II) phthalocyanine (**6**)	phenol	1,4-dihydroxybenzene (85 %)	NaOH, $(NH_4)_2S_2O_8$, 45 ℃, 10 h	oxidation	12

The integration of porphyrin and phthalocyanine nanomaterials in catalysis aligns with the principles of green chemistry, non-toxic reagents, and energy-efficient processes. Additionally, these materials are often reusable and stable, addressing the economic and environmental concerns associated with traditional catalysts. Therefore, we aim to explore the catalytic potential of porphyrin and phthalocyanine-based nanomaterials in organic transformations. Different nanocomposites of porphyrin and phthalocyanine to highlight their structural advantages, functional versatility, and applications in achieving sustainable chemical synthesis. These insights will pave the way for their expanded use in industrial and environmental applications.

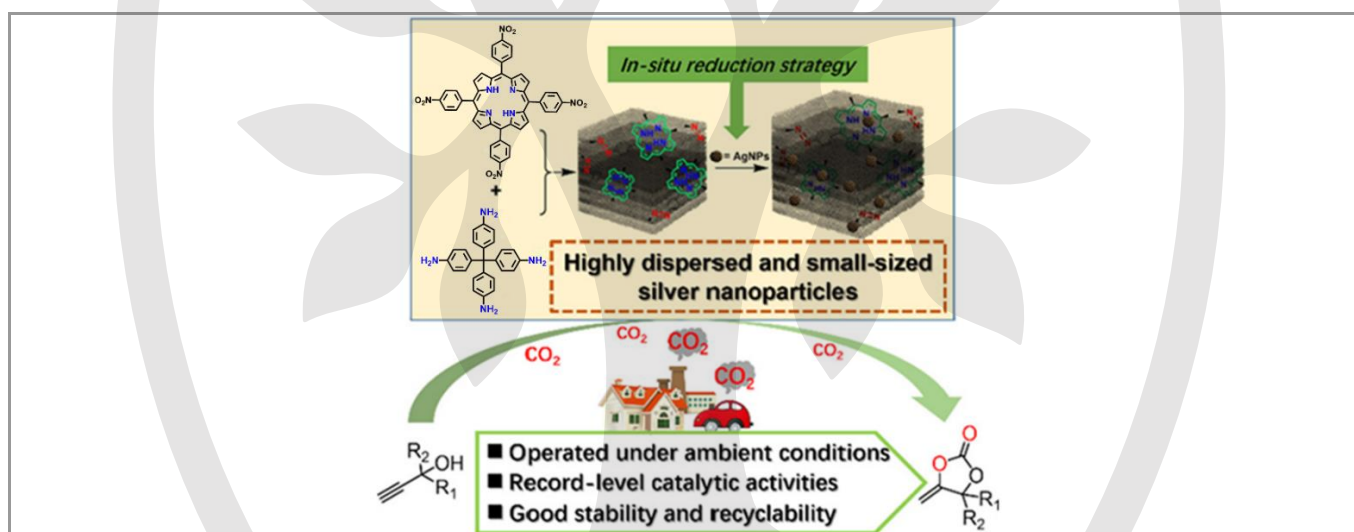## 2. Porphyrin and phthalocyanine-based nanocomposites for catalytic applications

Incorporating nanomaterials has significantly improved the catalytic activity and stability of porphyrin and phthalocyanine (Pc).[13] Nanomaterials possess a high surface-to-volume ratio and an extensive surface area, which enhances the reactivity of surface atoms and allows for effective interaction with porphyrin and Pc.[14] Various nanomaterials, including nanoparticles of gold, silver, palladium, platinum, and metal oxides like iron, titanium, and zinc, as well as carbon nanomaterials such as graphene oxide, carbon nanotubes, graphitic carbon nitrite, have been utilized to modify porphyrin and Pc through both covalent and non-covalent bonding. Porphyrin-based nanoporous organic frameworks have recently shown remarkable catalytic activity due to their high surface area, porosity, and stability, making them widely applicable in organic transformations.[15] Porphyrin and Pc-based nanocomposites and nanoporous organic frameworks are advantageous for catalytic transformations in organic reactions due to their ability to produce high yields, exhibit excellent atomic economy, and strong recycling capabilities while minimizing the formation of by-products. Furthermore, these nanocomposites are generally less toxic to the environment. The subsequent sections explore the various types of porphyrin and phthalocyanine-based nanocomposites and their catalytic activities.

2.1 Porphyrin and phthalocyanine-based nanocomposites with metal nanoparticles

Metal nanoparticles, typically ranging from 1 to 100 nanometres in size, are recognized for their large surface area, which significantly enhances their reactivity and effectiveness as catalysts in various organic reactions.[16] The increased surface area provides more active sites for chemical interactions, making them effective catalysts due to their size-dependent properties. However, despite these benefits, metal nanoparticles face challenges related to stability and the tendency to agglomerate, which can adversely affect their catalytic performance by reducing the available surface area and active sites.[17] Metal nanoparticles have been modified with porphyrin and Pc to overcome these challenges. The porphyrin/Pc-metal nanocomposites enhance the stability and dispersion of the nanoparticles, preventing agglomeration and ensuring the availability of an enormous number of active sites for catalysis.[18,19] Additionally, porphyrin and Pc can facilitate electron transfer processes, improving their catalytic efficiency. The porphyrin/Pc-metal nanocomposites also allow better control over the reaction conditions, resulting in increased selectivity and reusability of the catalyst. Overall, this synergistic effect leads to a more robust and effective catalytic system, surpassing the performance of metal nanoparticles used independently.

Recently, Yang et al. fabricated a silver nanoparticle (AgNPs)-supported azo-bridged porous porphyrin framework (Ag/Azo-Por-TAPM) through a simple "liquid impregnation and in situ reduction" strategy (Scheme 1).[20] Strong interactions between the AgNPs and nitrogen sites on the composite's surface prevented the nanoparticles from aggregating and leaching. Due to these unique structural characteristics, Ag/Azo-Por-TAPM demonstrated remarkable catalytic activity and good recyclability, particularly in the synthesis of α-alkylidene cyclic carbonates by utilizing CO_2 and propargylic alcohols reaching maximum turnover frequencies of 1050 h^{-1} at 1 bar and 4600 h^{-1} at 10 bar of CO_2 pressure at room temperature. This method offered an atom-economical approach to utilize CO_2 (Scheme 1).[20] These advancements highlight the synergistic effects of porphyrins combined with metal nanomaterials, leading to catalysts that show enhanced activity and selectivity and maintain stability under various reaction conditions. Overall, this research underscores the transformative potential of these materials in promoting sustainable chemical processes through advanced catalysis. Due to high catalytic activity, many scientists have used the porphyrin/Pc-metal nanocomposite in different organic reactions, including oxidation, reduction, and Suzuki-Miyaura coupling (Table 2).

Scheme 1 Silver nanoparticle-supported azo-bridged porous porphyrin framework (Ag/Azo-Por-TAPM) utilized as a catalyst in the synthesis of α-alkylidene cyclic carbonates (adapted with permission from reference[20]. Copyright 2024 American Chemical Society

Table 2 Porphyrin and phthalocyanine-based metal nanoparticles nanocomposites used in different organic reactions as catalysts

Entry	Catalyst	Reactant	Product (Yield)	Reaction Conditions	Reaction type	Reference
1	Tantalum (V) phthalocyanines@AuNPs	cyclohexene	cyclohexenol (7 %), cyclohexene-one (17 %) cyclohexene oxide (9 %) cyclohaxanediol (6 %)	RT, 180 min., toluene solvent	photocatalytic oxidation	[21]
2	Au@CPF-1	4-nitrophenol	4-aminophenol (>99 %)	$NaBH_4$, water, 12 min.	reduction	[22]
3	Ru-TPP-CH$_2$S-AuNPs	phenylacetylenes	1-phenylnapthalene (64 %), 1,2,3-triphenylbenzene (2 %), 1,2,4-triphenylbenzene (10 %), 1,3,5-triphenylbenzene (26 %)	48 h	oligomerization	[23]

4	Polymeric TPP@AuNPs	alkyne	corresponding aldehyde and ketone (99-75 %)	propionic acid, H$_2$O, 80 ℃, 3 h	oxidation	[24]
	Polymeric TPP@AuNPs	alcohol	corresponding aldehyde and ketone (99-96 %)	K$_2$CO$_3$, H$_2$O, RT, 24 h	oxidation	
5	Pd NPs@TPP	4-nitrophenol	4-aminophenol (>99 %)	NH$_3$BH$_3$ CH$_3$OH, H$_2$O, RT, 2 min.	hydrogenation/ reduction	[25]
6	Pd@PPPP	phenylboronic acid and iodobenzene	biaryls (92 %)	p-xylene, K$_2$CO$_3$, 150 ℃, 3 h	Suzuki-Miyaura coupling	[26]

CPF-1: hexagonal porphyrin-based porous organic polymer; TPP: triphenyl porphyrin; PPPP- porphyrin(5,10,15,20-tetrakis(4-aminobiphenyl)porphyrin)-based porous polyimide polymers
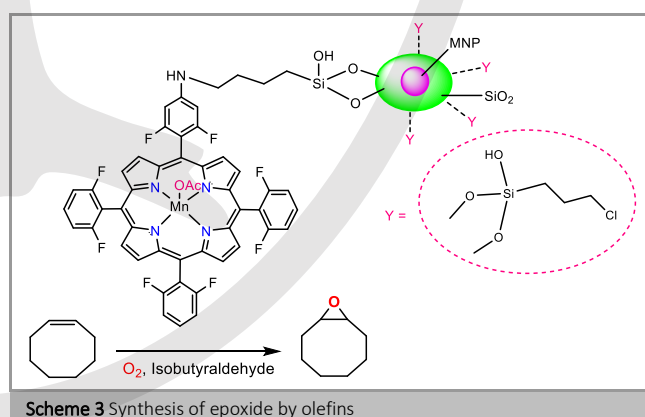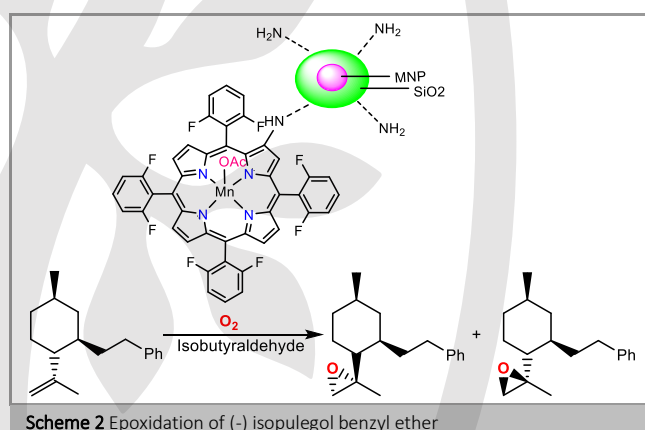
2.2 Metal oxide nanoparticles modified porphyrin and phthalocyanine nanocomposites

2.2.1 Nanoconjugates of porphyrin and phthalocyanine with magnetic nanoparticles

Magnetite nanoparticles (Fe$_3$O$_4$, MNPs) exhibit unique properties such as a large surface area, magnetic separability, and notable catalytic activity.[27–32] However, their susceptibility to oxidation in the presence of moisture compromises their stability. This limitation can be addressed by coating the nanoparticles with a silica layer, which enhances their stability and facilitates covalent bonding with other compounds.[33] The resulting improvement in stability is vital for maintaining catalytic performance over multiple reaction cycles. Their catalytic efficiency is significantly enhanced when silica-coated MNPs are combined with porphyrin or Pc. This enhancement arises from improved stability, larger surface area, water dispersibility, and ease of recovery *via* an external magnet, creating an effective heterogeneous catalyst.[34,35] These hybrid materials demonstrated unique properties from the individual components. Furthermore, the porphyrin/Pc-based MNPs accelerate organic reactions by increasing the active sites, promoting electron transfer, and reducing activation energy, thereby achieving higher reaction rates.[36]

Pereira et al. synthesized a nanocomposite by grafting 2-nitro-5,10,15,20-tetrakis(2,6-fluorophenyl)porphyrinatomanganese(III) acetate (NH-TDFPP-Mn(III)) onto silica-coated MNPs, resulting in the formation of an MNP@SiO$_2$-NH-TDFPP-Mn(III) nanocomposite.[36] This nanocomposite demonstrated high stability, activity, and selectivity during the epoxidation of (−)-isopulegol benzyl ether in the presence of molecular oxygen and isobutyraldehyde, yielding diastereoisomers of (−)-isopulegol benzyl epoxide, which have potential applications as anticancer agents (Scheme 2). Additionally, they synthesized a similar nanocomposite using 5-(4-aminophenyl)-10,15,20-tri-(2,6-chlorophenyl)porphyrinato manganese(III) (4-NH-Mn-TDCPP) supported on silica-coated MNPs, which was employed in the selective epoxidation of olefins in the presence of molecular oxygen and isobutyraldehyde as a co-reductant (Scheme 3).[37] The nanocomposite was recyclable for up to five cycles without losing its efficiency.

The catalytic activity of porphyrin/MNPs can be further enhanced by incorporating ZnO NPs. Rabbani et al. synthesized a TCPP/Zn-Fe$_2$O$_4$/ZnO nanocomposite, which exhibited 96% conversion and 100% selectivity for oxidizing benzyl alcohol to benzaldehyde.[38] This conversion rate was 1.55 times greater than TCPP/Zn-Fe$_2$O$_4$, highlighting the role of ZnO in improving catalytic efficiency. The distinctive properties of magnetic porphyrin/Pc-based nanomaterials have drawn scientists' attention, and these nano-catalysts have been utilized in various oxidation, addition, and condensation reactions (Table 3).

Scheme 2 Epoxidation of (-) isopulegol benzyl ether

Scheme 3 Synthesis of epoxide by olefins

Table 3 Porphyrin and phthalocyanine-based MNPs as catalysts in the organic reaction under different conditions

Entry	Catalyst	Reactant	Product (Yield)	Reaction conditions	Reaction Type	Reference

1	Poly-Fe$_3$O$_4$@SiO$_2$@(CH$_2$)$_3$-GO-[PTTA-NH-Ni]	2,4-thiazoli-dinedione, aldehydes, malononitrile, and ammonium acetate	5-amino-7-aryl-2-oxo-2,3-dihydrothiazolo[4,5-b]pyridine-6-carbonitriles (90 %)	75 ℃, 10 min.	condensation	39
		aldehydes, acetophenones, and 3-amino-1,2,4-triazole	7-diaryl-4,7-dihydro-[1,2,4]triazolo[1,5-a]pyrimidine (92-82 %)			
2	[Fe$_3$O$_4$@SiO$_2$@NH$_2$@MnTCPP(OAc)	olefins	epoxide (100-67 %)	acetone, O$_2$ (1atm), RT, 30 min.	oxidation	40
3	MNP-P	propylene oxide, CO$_2$	cyclic carbonate (97 %)	PTAT, CO$_2$ (1 MPa), RT, 24 h	cycloaddition	41
4	MnP3-NH-SBA-Si-Mag	*cis*-cyclooctene	*cis*-cyclooctene oxide (77 %)	PhIO, RT, 1 h	oxidation	42
5	(MNPs)-(BTSE)-(COOH-POPP)	benzaldehyde, malononitrile	benzylidene malononitrile (88 %)	anhydrous ethanol, RT, 30 min.	Knoevenagel condensation	36
6	MNP@SiO$_2$ [4-NHMnTDCPP]	alkene	epoxide (96-57 %)	O$_2$ bubbling, isobutyraldehyde, butyronitrile solvent, RT, 2 h	oxidation	43
7	Fe$_3$O$_4$@SiO$_2$-NHCO-NH$_2$-MnTCPP	alkene	epoxide (99-18 %)	molecular oxygen, IBA, acetone, 38 ℃, 2 h	oxidation	44
8	Fe$_3$O$_4$@SiO$_2$ N$_3$@[MnTHPP]	alkene	epoxide (85-44 %)	TBHP, dichloroethane, 75 ℃, 12 h	oxidation	35
9	Fe$_3$O$_4$ /SiO$_2$ MnTCPP(OAc)	sulfide	sulfoxide (99-68 %)	UHP, ImH, ethanol, acetic acid, RT, 3.5 h	oxidation	45
10	Fe$_3$O$_4$/SiO$_2$/NH$_2$-Fe(TCPP)Cl	cyclooctene	epoxide (97%)	ImH, CH$_3$CN, H$_2$O$_2$, RT, 5 h	oxidation	46
11	Fe$_3$O$_4$/SiO$_2$/NH$_2$-Mn(TCPP)OAc	cyclooctene	epoxide (87%)	ImH, CH$_3$CN, H$_2$O$_2$, RT, 5 h	oxidation	46
12	MNP@SiO$_2$-NH-TDFPP-Mn(III)	(-)-isopulegol benzyl ether	diasteriosomer of (-)-isopulegol benzyl ether epoxide (51 %, and 45 %)	IBA, butyronitrile, O$_2$ (5 bar), 25 ℃, 6 h	oxidation	47
13	Fe$_3$O$_4$–MnCP@SiO$_2$	ethylbenzene	hypnone (with 75 % selectivity)	O$_2$ bubbling (1 atm), 100 ℃, 10 h	oxidation	48
14	Fe$_3$O$_4$@SiO$_2$-Im@[MnT(4-OMeP)P]	alkene	epoxide (88 -61 %)	n-Bu$_4$NHSO$_5$, DCM, 20 h	oxidation	49
		sulfide	sulfoxide (70 %)	UHP, DCM, RT, 20 h		
15	Fe$_3$O$_4$@Fe(TPP)Cl	sulfide	sulfoxide (96-78 %)	m-CPBA, 10 ℃, 10 min.	oxidation	50
16	Fe$_3$O$_4$@SiO$_2$@[Mn(Br$_2$TPP)OAc]	alkene sulfide	epoxide (95-60 %) sulfoxide (95-87 %)	n-Bu$_4$NHSO$_5$, 70 ℃, 45 min., for sulfoxidation at RT	oxidation	51
17	Fe$_3$O$_4$@SiO$_2$@SiO$_2$(CH$_2$)$_3$-NH-ACoPc	aldehyde, malononitrile, and dimedone	tetrahydrobenzo[b]pyran (97-90 %)	RT, 15 min.	condensation	52
18	Fe$_3$O$_4$@SiO$_2$@SiO$_2$(CH$_2$)$_3$-NH-AVOPc	2,5-dimethoxybenzaldehyde, malononitrile, 4-hydroxycoumarin	2-amino-4-aryl-5-oxo-4H,5H-pyrano[3,2-c]chromene-3-carbonitrile (92 %)	75 ℃, 20 min.	cycloaddition	53
19	Fe$_3$O$_4$@SiO$_2$-GA-Cu(Pc)	4-chlorobenzaldehyde, acetophenone, acetonitrile	β-amido ketones (91 %)	acetyl chloride, 50 ℃, 1.5 h	coupling	54

20	CoPcS@ASMNP	mercaptans	disulfide (96-35 %)	molecular oxygen, H₂O, 70 ℃, 2-12 h	oxidation	[55]
21	CuPcS@ASMNP	alkene,	epoxide (96-40 %)	n-Bu₄NHSO₅, 70 ℃, 90 min.	oxidation	[56]
		hydrocarbon	aldehyde and ketone (90-12 %)	n-Bu₄NHSO₅, 90 ℃, 150 min.		
		sulfide	sulfoxide (97-70 %)	RT, 60 min.		
22	TCPP/Zn–Fe₂O₄@ZnO	alcohol	aldehyde and ketone (96-44 %)	H₂O₂, CH₃CN, 80 ℃, 1.5-2 h	oxidation	[38]
23	CoPc/nano ZnO	alcohol	aldehyde and ketone (84-63 %)	TBHP, reflux temp., 8 h	oxidation	[57]

PTTA: 4,4′,4″,4‴-(porphyrin-5,10,15,20-tetrayl)tetraaniline; TCPP: Meso-tetrakis(4-carboxyphenyl)porphyrin; MNP-P: magnetic nanoparticle-supported porphyrinato cobalt[III]; PTAT: phenyltrimethylammonium tribromide; SBA-Si-Mag: MNPs coated by amorphous silica and mesoporous silica SBA-15 using Pluronic 123; MnP3: [5,10,15,20-tetrakis (pentafluoridephenylporphyrin) manganese (III); PhIO: iodosylbenzene; BTSE: bis(triethoxysilyl)ethane; COOH-POPP: 5-(4-carboxyphenyl)-5,10,15-tris(4 phenoxyphenyl)-porphyrin; NHMnTDCPP:5-(4-aminophenyl)-10,15,20-tri(2,6-dichlorophenyl)porphyrinatomanganese; IBA: isobutyraldehyde; TBHP: tert-butylhydroperoxide; THPP: mesotetrakis(4-hydroxyphenyl)porphyrin; UHP: urea hydrogen peroxide; ImH: imidazole; TDFPP: 5,10,15,20-tetrakis(2,6-difluorophenyl) porphyrin; MnCP: Manganese (III) 5-(p-carboxyphenyl)-10,15,20-triphenylporphyrinchloridize; n-Bu₄NHSO₅: tetra-n butylammonium hydrogen monopersulfate; [T(4-OMeP)P]: meso-tetrakis(4-methoxyphenyl)porphyrin; m-CPBA: Meta-Chloro Peroxy Benzoic Acid; TPP: 5,10,15,20-tetrakis(4-phenyl)porphyrin; ACoPc: Amino cobalt phthalocyanine; AVOPc: Amino vanadium(II)oxide phthalocyanine; GA: guanidine; CoPcS@ASMNP: silica coated magnetic nanoparticles immobilized cobalt phthalocyanine.
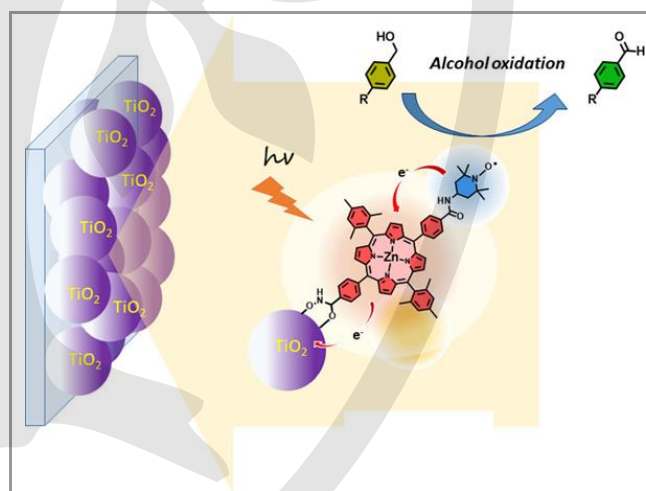
2.2.2 Nanocomposites of porphyrin and phthalocyanine with titanium oxide nanoparticles

Titanium dioxide nanoparticles (TiO₂ NPs) have been explored in various photocatalytic transformations. TiO₂ NPs demonstrate high stability, photoactivity, non-toxicity, and a large surface area. However, their large band gap only limits their activity to the UV region.[58,59] To overcome this limitation, the photocatalytic performance of TiO₂ has been improved by coupling it with photoactive compounds like porphyrins and Pc. These porphyrin/Pc-TiO₂-based nanomaterials exhibited high catalytic activity under visible light due to a narrow band gap and synergistic effects.[60]

Upon exposure to visible light, porphyrin/Pc units present in nanocomposites absorb light due to its reduced band gap, facilitating electron excitation from the highest occupied molecular orbital (HOMO) to the lowest unoccupied molecular orbital (LUMO). Thereafter, electrons transition from the LUMO to TiO₂'s conduction band takes place.[61] These excited electrons can generate reactive radical species to catalyze the various reactions. For instance, the excited electrons can be captured by oxygen and carbon dioxide, forming radical species. Oxygen generates superoxide radicals, which drive oxidation reactions,[60] while carbon dioxide is reduced to produce formic acid, methanol, and formaldehyde. The low recombination rate of electrons and holes significantly increases the photo efficiency.[61]

Hong et al. synthesized a CoPc/TiO₂ nanorod-based composite for the selective oxidation of quinoline to quinclorac.[62] The CoPc/TiO₂-2.5%-Mn-Br variant achieved 92 % selectivity for quinclorac with 86 % yield, which was 2.43 times greater than the CoPc-Mn-Br. Quinclorac is a versatile organic compound that is crucial as a precursor in multiple domains, including agriculture, pharmaceuticals, and synthetic chemistry.

Similarly, Vauthey et al. developed a nanocomposite using Zn(II)porphyrin, TiO₂ NPs, and 2,2,6,6-tetramethyl-1-piperidine N-oxyl (TEMPO). This nanocomposite was employed in the oxidation reaction of benzyl alcohol to benzylaldehyde within Dye-Sensitized Photoelectrosynthesis Cells (Scheme 4).[63] TEMPO is an environmentally friendly, effective catalyst for selective alcohol oxidation, and its combination with the nanocatalyst synergistically enhanced the nanocomposite's catalytic activity.[64] Numerous researchers have utilized porphyrin/phthalocyanine-TiO₂-based nanomaterials for oxidation and reduction reactions, showcasing their versatility and effectiveness (Table 4).

Scheme 4 TiO₂/ZnP/TEMPO nanocomposite use in alcohol oxidation in Dye-Sensitized Photo electrosynthesis Cells (Reproduced with permission from reference[63]. Copyright 2021 American Chemical Society)

Table 4 Porphyrin and phthalocyanine

@TiO₂-based nano-catalysts employed in the organic reaction under light irradiation

Entry	Catalyst	Reactant	Product (yield)	Reaction condition	Reaction Type	Reference
1	TCPP-TiO₂	famotidine	famotidine-S-oxide (>99 %)	hv>400 nm, 3 h	photooxidation	[65]

2	ZnPy–TiO$_2$	CO_2	CO/CH$_4$ (8/1 µmol g^{-1} h^{-1})	λ≥420 nm, 2 h	photoreduction	[66]
3	Co–TCPP@TiO$_2$/BiVO4	benzyl alcohol	benzaldehyde (85 %)	λ=550 nm, TBHP, CH$_3$CN, 70 ℃, 60 min.	photooxidation	[60]
4	ZnPyP–RuBiPy–TNT	CO_2	methanol (687 µmol (g cat)$^{-1}$)	0.82 W/cm^2, CO_2 purge, 5 h	photoreduction	[67]
5	Co-TCPP@TiO$_2$/WO$_3$	benzyl alcohol	benzaldehyde (86 %)	LED light (5 W), CH$_3$CN, 30 ℃, 60 min.	photooxidation	[68]
7	ZnTCPP-TiO$_2$/CoFe$_2$O$_4$	benzyl alcohol	benzaldehyde (82 %)	H$_2$O$_2$, 120 min.,	photooxidation	[69]
8	NiTCPP-TNT	CO_2	CH$_4$ (reduction rate - 33 µmol cm^{-2} h^{-1})	500 W xenon lamp, 0.2 V, CO_2 purge with water (60 mL/min.)	photoreduction	[70]
9	TAPP@SiO$_2$-TiO$_2$ nanosphere	Sulfide	sulfoxide (98 %)	O$_2$ (1 atm), H$_2$O, xenon lamp	photooxidation	[71]
10	Mn(TMPIP)/TiO$_2$	Sulfide	sulfoxide (98 %)	IBA, O$_2$(1 atm), toluene, 20 ℃, 3 h	oxidation	[72]
11	CoPc/TiO$_2$-2.5%-Mn-Br	3,7-dichloro-8-dichloro methyl quinoline	quinclorac (91 %)	O$_2$ (4 MPa), 160 ℃, acetic acid, 6 h	oxidation	[62]
12	CoPc/TiO$_2$	CO_2	formic acid (1487 µmol (g cat)$^{-1}$)	visible light (500 W), 10 h	photoreduction	[61]
13	ZnPc/TiO$_2$	CO_2	methanol (248 µmol (g cat)$^{-1}$)	xenon arc lamp (500 W), 8 h	photoreduction	[73]
14	3%CoPc-TiO$_2$	CO_2	formic acid (2863 µmol (g cat)$^{-1}$)	visible light, 20 h	photoreduction	[74]
15	Ru-CoPc@TiO$_2$@SiO$_2$@Fe$_3$O$_4$	CO_2	methanol (2570 µmol (g cat)$^{-1}$)	visible light, 48 h, triethylamine	photoreduction	[75]
16	FePc/Au-TiO$_2$	5-hydroxymethylfurfural	2,5-furandicarboxylic acid (97 %)	visible light, NaOH, 15 h	photo-oxidation	[76]
17	CoPc-TiO$_2$	CO_2	formic acid (82660 µmol (g cat)$^{-1}$)	visible light, NaOH, 10 h	photoreduction	[77]
18	CoPc/TiO$_2$	CO_2	formic acid, CO, aldehyde, methanol (total conversion-406 µmol (g cat)$^{-1}$)	LED bulb (500 W), NaOH, 20 h	photoreduction	[78]
19	CuPc/TiO$_2$/rGO	methyl methacrylate	polymer of methyl methacrylate (90 %)	visible light, RT, 24 h	polymerization	[79]
20	TiO$_2$-ZnP–TEMPO	benzyl alcohol	benzaldehyde (76 % FE)	electrochemical	Oxidation	[63]

TCPP-tetra(4-carboxyphenyl)porphyrin; Py:pyridine based porphyrin; TBHP: tert-butylhydroperoxide; ZnPyP–RuBiPy–TNT: µ-meso-[(5,10,15,20-tetra-4-pyridylporphyrinato) zinc (II)] tetrakis [chloro-2,29-bipyridylruthenium(II)] tetrahexafluorophosphate-TiO$_2$ nanotube; TMPIP: 2-arylimidazo[4,5-b]porphyrin; IBA: isobutyraldehyde; Cu(II)Pc: Cu(II) tetrakis[4-(2,4-bis-(1,1-dimethylpropyl)phenoxy)]phthalocyanine, FE- faradic efficiency.

2.3 Porphyrin and phthalocyanine-based nanocomposites with carbon-based nanomaterial

2.3.1 Porphyrin and phthalocyanine nanocomposites with carbon nanotubes

Carbon nanotubes (CNTs) are nanoscale structures resembling hollow tubes created by rolling a graphite sheet.[80] These materials possess distinctive features, including a large surface area, excellent conductivity, high mechanical strength, low density, efficient electron transfer capabilities, and remarkable thermal and chemical stability.[81] CNTs are categorized based on the number of carbon walls into single-walled carbon nanotubes (SWCNTs), double-walled carbon nanotubes (DWCNTs), and multi-walled carbon nanotubes (MWCNTs).[80] Among these, MWCNTs are favored for reactions due to their ease of synthesis, high purity, and better dispersibility. Their exceptional properties and limited solubility make MWCNTs suitable as solid support for porphyrin or Pc, which enhance the catalytic performance of hybrid systems through synergistic effects.[82] These hybrids act as heterogeneous catalysts, with CNTs and porphyrin/Pc interacting through electrostatic and covalent bonding. Due to the remarkable features of porphyrin/Pc@CNT-

based nanocomposites, it has been used in different organic transformations. These nanocomposites also utilize electrochemical synthesis because of their high electron transfer capability (Table 5).
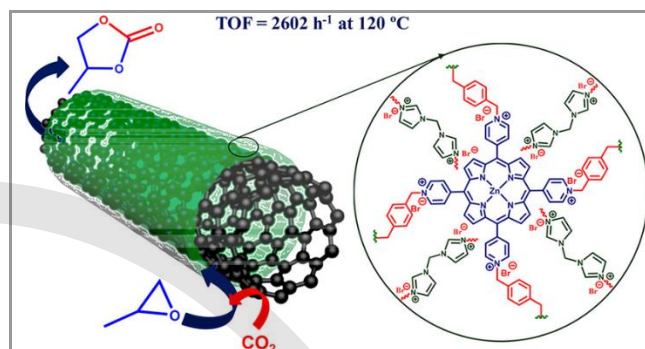
In a study, Chen et al. reported the conversion of levulinic ester into γ-valerolactone (GVL) and pyrrolidone derivatives in the presence of polymeric Ru-porphyrin (RuPP)/CNTs catalyst (Scheme 5).[83] GVL is an efficient solvent in biomass conversion, while pyrrolidone serves multiple roles, including surfactant, solvent, and complexing agent. Ru-porphyrin demonstrated good catalytic activity in the organic reactions but couldn't be recovered. Ru-porphyrin was electrostatically linked to CNTs to improve catalytic activity and recoverability. The RuPP/CNTs catalyst facilitated the synthesis of GVL from levulinic ester as well as the production of pyrrolidone through the reduction of ethyl levulinate with various amines, achieving a yield of 96 to 88 % for pyrrolidone and >99% for GVL. The RuPP/CNT catalyst maintained its efficiency over five reusability cycles.

Similarly, Yang et al. developed a ZnTPy-BIM4/CNTs-3 nanocomposite by treating 5,10,15,20-tetrakis(4-pyridyl)porphyrin zinc(II) with 1,4-bis(bromomethyl)-benzene (BBM br), and di(1H-imidazol-1-yl)methane (MBIM). The cationic Zn(II)porphyrin polymer was attached to CNTs through the electrostatic interaction (Scheme 6).[84] This nanocomposite was employed in a cycloaddition reaction involving CO_2 and epoxide at 120 ℃ without a co-catalyst. The study revealed a synergistic effect among the components; the yield of cyclic carbonate product was 64%, 76%, and 98% for ZnTPy, ZnTPy-CNTs-3, and ZnTPy-BIM4/CNTs-3, respectively, at CO_2 pressure of 1.5 MPa, 120 ℃ temperatures in 2.5 hours reaction time.
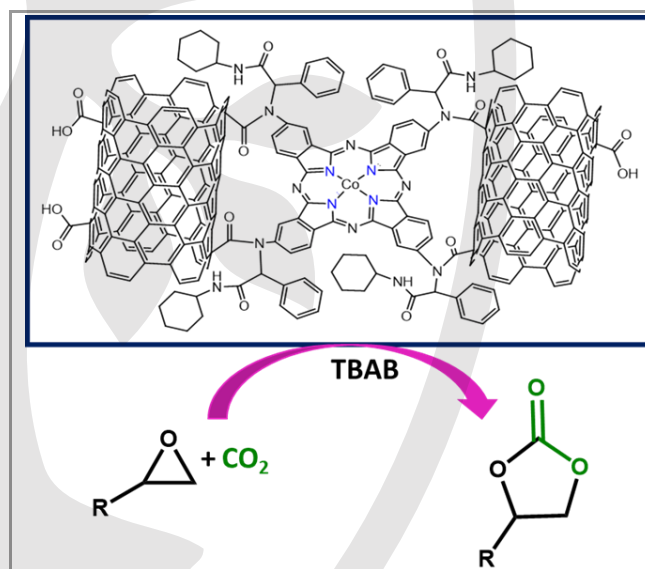

Scheme 6 Production of cyclic carbonate by using CO_2 and epoxide in the presence of ZnTPy-BIM4/CNTs-3 nanocomposite (Reproduced with the permission from reference[84], Copyright 2018 American Chemical Society

In another study, Shaabani et al. synthesized a CoPcTA/MWCNTs nanocomposite through a four-component Ugi reaction involving tetra-amino cobalt phthalocyanine (Co-PcTA), cyclohexyl isocyanide, benzaldehyde, and MWCNT utilizing covalent interaction (Scheme 7).[85] This catalyst was applied in a cycloaddition reaction with CO_2 (2.5 bar), 80℃ for 1 hour, using tetrabutylammonium bromide (TBAB) as a co-catalyst. The yield of cyclic carbonate was >93% for various epoxides. The catalyst demonstrated high efficiency across seven recycling experiments, indicating that the porphyrin/Pc-MWCNTs-based nanocomposite exhibited significant catalytic activity and was easily recoverable after the reaction.

Scheme 5 Synthesis of γ-valerolactone and pyrrolidone by using polymeric Ru(II)porphyrin/CNTs nanocomposite

Scheme 7 CoPcTA/MWCNTs nanocomposite used in the cycloaddition reaction

Table 5 Porphyrin and phthalocyanine@CNT-based catalysts used in the organic transformations

Entry	Catalyst	Reactant	Product (Yield)	Reaction Condition	Reaction Type	Reference
1	Mn(TAPP)Cl@MWCNT	imidazolines	imidazoles (86 %)	$NaIO_4$, CH_3CN/H_2O, ultrasonic irradiation, 40 ℃, 10 h	oxidation	[86]
2	Fe(THPP)Cl@MWCNT	olefins	epoxide (56 % conversion with 10 % selectivity)	TBHP, CH_3CN, RT, 24 h	oxidation	[87]

3	Fe(THPP)Cl@MWCNTs]	olefins	epoxide (100 %)	IBA, O_2 (1 atm), CH_3CN, RT, 60 min.	oxidation	[88]
4	[Fe(TPP)Cl]@AMWCNT	olefins	epoxide (100 %)	n-Bu$_4$NHSO$_5$, 70 ℃, 15 min.	oxidation	[89]
		sulfide	sulfones (95 % conversion with 98 % selectivity)	water, air, RT, 20 min.		
		sulfide	sulfoxide (92 %)	ethanol, air, 30 min., RT		
5	Fe(TCPP)Cl@MWCNT	sulfide	sulfoxide (38 %)	UHP, water, air, RT, 90 min.	oxidation	[90]
6	FeP@MWCNT	*cis*-cyclooctene	epoxide (95 % conversion)	H_2O_2 aq., ethanol, RT, 5 h	oxidation	[91]
7	[Mn(TAPP)Cl-MWCNT	alkenes	epoxide (95 %)	CH_3CN/H_2O, NaIO$_4$, ImH, RT, 2 h	oxidation	[92]
8	Mn(THPP)OAc@MWCNT	olefins	epoxide (100 % conversion with 76 % selectivity)	IBA, ImH, CH_3CN, RT, 2 h	oxidation	[93]
9	Fe(THPP)Cl@MWCNT	alkene	epoxide (50 %)	H_2O_2, ethanol, Ultrasonic waves 60 min.	oxidation	[94]
10	Mn(THPP)OAc@MWCNT	alkene	epoxide (100 %)	H_2O_2 aq, ImH, acetic anhydride, 30 min., ultrasonic irradiation	oxidation	[95]
11	FeTPy-MWCNT	CO_2	CH_4 (92 % FE)	electrochemical	reduction	[96]
12	MWCNT-TSP-AlCl-imi	epoxide, CO_2	cyclic carbonate (55 %)	CO_2 (25 bar), 125 ℃, 3 h	cycloaddition	[97]
13	Mn(THPP)OAc@MWCNT	olefins	epoxide (82 %)	UHP, acetic anhydride, RT, 4 h	oxidation	[98]
14	RuPP/CNT	ethyl levulinate, amine	pyrrolidone (99 %)	THF, H_2 (3 MPa), 120 ℃, 24 h	reductive amination	[83]
15	Mn(TCPP)OAc@MWCNT	2,6-dimethylphenol	quinone (86 %)	TBHP, ImH, phenol, CH_3CN, RT, 5 h	oxidation	[99]
16	Mn(TAPP)Cl@MWCNT	α-aryl carboxylic acids	aldehyde and ketone (97-89 %)	NaIO$_4$, ImH, CH_3CN/H_2O, RT, 50-110 min.	decarboxylation	[100]
		alkane	ketone (86 %)	NaIO$_4$, ImH, CH_3CN/H_2O, 2 h	hydroxylation	
17	Cationic polymer of ZnTPy- BIM4/CNT-3	epoxide, CO_2	cyclic carbonate (98-51 %)	CO_2 (1.5 MPa), 120 ℃, 2.5-24 h	cycloaddition	[84]
18	T(o-Cl)PPCu-AMWCNT	alkyne, epoxide, sodium azide	triazole (93-78 %)	H_2O, RT, 0.8-2.8 h	cycloaddition	[101]
19	CoTPP@CNT	ethylbenzene	acetophenone (19 % conversion with 72 % selectivity)	O_2 (0.8 MPa), 120 ℃, 5 h	oxidation	[102]
20	MnTPy(OAc)@MWCNT	alkene	epoxide (86-10 %)	ethanol, H_2O, ImH, Acetic acid, Oxone®, RT, 5-90 min.	oxidation	[103]
21	Mn(THPP)OAc@MWCNT	aldehyde	alcohol (100 %)	ImH, NaBH$_4$, CH_3OH, RT, 2-5 min.	reduction	[104]
		Ketone	alcohol (100 %)	ImH, NaBH$_4$, CHCl$_3$, ethanol, 0 ℃, 5-40 min.		
22	CuPOF-Bpy/Cu$_2$O@CNT	CO_2	C_2H_4 (71% FE)	electrochemically	reduction	[105]
23	TPy/CNT	thioether	sulfoxide (100 %)	tris Buffer, LED light, Air (1 atm), RT, 1.5-4 h	photooxidation	[106]
24	ZnTImP-CP/ CNTs	epoxide, CO_2	cyclic carbonate (99-12 %)	CO_2 (1.5 MPa), 120 ℃, 5-6 h	cycloaddition	[107]
25	Fe(THPP)Cl/MWCNT	alcohol	aldehyde and ketone (100-76 %)	IBA, O_2 (1 atm), 45 ℃, 3 h	oxidation	[108]
26	MWCNT-TSP-Mg-imi	epoxide, CO_2	cyclic carbonate (95-32 %)	CO_2 (25 bar), 100-150 ℃, 3-24 h	cycloaddition	[109]

27	Mn/Fe (THPP)@MWCNT	α- methyl styrene	ketone (81% conversion with 62 % selectivity)	O_2 (1 atm), 110 ℃, 10 h	oxidation	[110]
		tetrahydronaphthalene	ketone, alcohol (30 % conversion)	O_2 (1 atm), 130 ℃, 8 h		
28	Mn(TCPP)OAc@MWCNT	cyclohexene	epoxide (TON= 2700)	ImH, O_2 (1 atm), CH_3CN, 25 ℃, 72 h	oxidation	[111]
29	MWCNT-H_2TCPP	cyclohexene	2-cyclohexene-1-one (97%)	sun light, CH_3CN, RT, 72 h	oxidation	[112]
		thioanisole	sulfoxide (52 % conversion)	light (40 W), RT, 43 h		
30	Fe (TCPP)Cl@MWCNT	alkene	epoxide (100% conversion)	IBA, O_2 (1atm), CH_3CN, 40-45℃, 1-4 h	oxidation	[113]
		cycloalkane	Cyclo ketone (50 % conversion)			
31	CoTCPP-CNT-NH_2	furfural	succinic acid (60 %)	O_2 (1 MPa), H_2O, 100 ℃, 20 h	oxidation	[114]
32	Sn^{IV}(TAPP)(OTf)$_2$@MWCNT	alcohol	tetrahydropyran ether (100 %)	DHP, THF, RT, 3-7 min.	tetrahydropyranylation	[115]
	[Sn^{IV}(TAPP)(BF$_4$)$_2$@MWCNT]					
33	Mn(THPP)OAc@MWCNT	sulfide	sulfoxide (91 %)	UHP, acetic anhydride, ethanol, RT, 30 min.	oxidation	[116]
34	ZnPc–MWCNTs	styrene	styrene oxide (94 % conversion with 90 % selectivity)	H_2O_2 aq., 60 °C, 8 h	oxidation	[117]
35	CoPc-TA-MWCNT	epoxide, CO_2	cyclic carbonate (97 %)	CO_2 (2.5 bar), TBAB, 80 °C, 1 h	cycloaddition	[85]
36	(OPh-p-Cl)CoPc-MWCNT	styrene	benzaldehyde (100 % conversion with 89 % selectivity)	TBHP, THF, 80 °C, 4 h	oxidation	[118]
37	(OPh-p-Cl)CuPc-MWCNT	benzyl alcohol	benzaldehyde (61 %)	TBHP, DMF, 60 °C, 8 h	oxidation	[119]
38	CoPc($OC_{10}H_{14}N$)$_4$/MWCNT	styrene	styrene oxide (97 %)	TBHP, DMF, 80 ℃, 7 h	oxidation	[120]
39	SnPc-8F@CNTs	CO_2	CO_2RR (91 % FE)	electrochemical	CO_2 electrolysis	[121]
40	CoPc@CNT	CO_2	CH_3OH (>40 % FE)	electrochemical	electroreduction	[122]
41	bi-FePc/MWNT	2-chloro-4-ethylamino-6-isopropylamino-1,3,5- triazine	2-hydroxy-4-ethylamino-6-isopropylamino-1,3,5-triazine (98 % FE)	electrochemical	dechlorination	[123]
42	CoPc/CNT	amine, CO_2	N-methylamine (7 % FE)	electrochemical	N-methylation	[124]
43	[3α-(OPh-t-Bu)-α-NO_2]ZnPc-MWCNTs	styrene	styrene oxide (96 %)	TBHP, DMF, 100 ℃, 8 h	oxidation	[125]
44	TBP-CoPc@Py-TEMPO@CNT	5-hydroxymethylfurfural	2,5-furandicarboxylic acid (90 % FE)	electrochemical	oxidation	[126]
45	CoPc/CNT	1,2-dichloroethane	ethylene (100 % FE)	electrochemical	dechlorination	[127]
46	[4α(OPh-t-Bu)CoPc]-MWCNTs	styrene	styrene oxide (87 %)	TBHP, DMF, 90 ℃, 10 h	oxidation	[128]
47	CoPc- MWCNTs/MO	2-butanol	2-butanone	20 ℃, 90 min.	oxidation	[129]

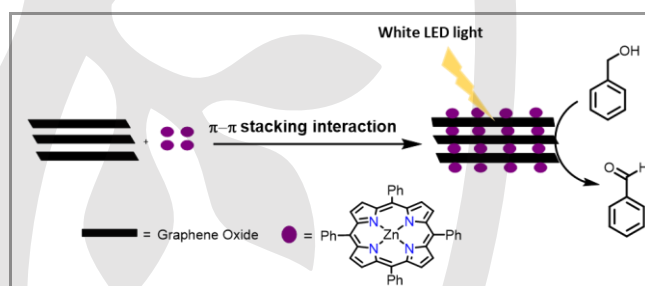| 48 | CoPc/CNT | CO_2 | methanol (10 % FE) | electrochemical | reduction | [130] |
49	CoPc/MWCNT	CO_2	methanol (36 % FE)	electrochemical	reduction	[131]
50	CuTNPc/MWCNTs	styrene	benzaldehyde (99 %)	TBHP, DMF, 90 ℃, 6 h	oxidation	[132]
51	CoPc/CNT	CO_2	methanol	electrochemical	reduction	[133]
52	CoPc SAC/SWCNTs	CO	ethylene	electrochemical	reduction	[134]
53	CoPc/CNT	2-chlorophenol	phenol (100 % FE)	electrochemical	dechlorination	[135]
54	CoPc/CNT	CO_2	methanol (40 % FE)	electrochemical	reduction	[136]
55	CoPc/CNT	ethylene	ethylene glycol (20 % FE)	electrochemical	oxidation	[137]

$NaIO_4$: Sodium periodate; TBHP: tert-butyl hydroperoxide; AMWCNT: activated multi-walled carbon nanotube; n-Bu_4NHSO_5: tetra-n butylammonium peroxomonosulfate; UHP: urea hydrogen peroxide; FeP: meso-tetrakis- (4-N,N-dimethylamine-2,3,5,6-tetrafluoro)porphyrinate iron(III) chloride; ImH: imidazole; IBA: Isobutyraldehyde; TPy:5,10,15,20-tetra-4-pyridylporphyrine; TSP-Al-Cl: aluminum chloride tetrastyrylporphyrin; imi:1,4-butanediyl-3,3′ -bis-1- vinylimidazolium dibromide; UHP: urea hydrogen peroxide; RuPP: polymeric rutheniumporphyrin; TBHP:tert -butyl hydroperoxide; MBIM: di(1H-imidazol-1-yl)methane; T(o-Cl)PPCu: meso-tetrakis(o-chlorophenyl)porphyrinato]copper(II); TPP: tetraphenyl porphyrin; POF: porphyrin organic framework; Bpy: bipyridine; ZnTImP: zinc 5,10,15,20-tetrakis(4-(imidazole)phenyl)porphyrin; CP: cationic polymer; TSP-Mg: magnesium tetrastyrylporphyrin; DHP: 3,4-dihydro-2H-pyran; TA: Tetra amino; SnPc-8F:2,3,9,10,16,17,23,24-octafluorophthalocyaninato tin (IV); TBP-CoPc: 4-(tert-butyl)-phenoxy-decorated cobalt phthalocyanine; Py-TEMPO: pyrene-tethered 2,2,6,6-tetramethylpiperidin-1-oxy; MO:Cr_2O_3-NiO; CuTNPc: tetranitro-copper phthalocyanine; SAC: Single atom catalyst

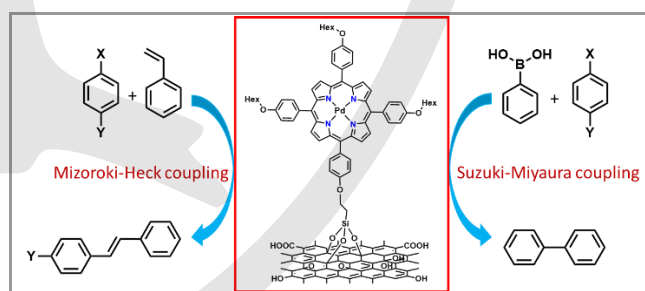## 2.3.2 Porphyrin/phthalocyanine-based nanocomposites with graphene oxide

Carbon-based nanomaterials, particularly graphene, are recognized as promising candidates in various applications due to their high stability, large surface area, excellent mechanical properties, and superior thermal and electrical conductivity.[138] However, they face some challenges, such as the tendency to agglomerate, complex synthesis processes, and hydrophobicity.[139] Modifications of the graphene surface are necessary to improve their catalytic performance. Graphene has been functionalized by oxygen-containing groups such as carboxylic acid, hydroxyl, and epoxide, resulting in graphene oxide (GO) exhibiting catalytic activity in various applications.[140–143] Due to its rich oxygen functionalities, GO demonstrates hydrophilicity and high catalytic activity. Covalent and non-covalent interactions with other catalytic active components can modify GO's properties for specific applications.[139] Porphyrin and PC compounds exhibit significant catalytic activity, but their recoverability poses a challenge. These compounds can be linked to GO through electrostatic and covalent interaction to improve stability. The resulting nanocomposites demonstrate high surface area, catalytic activity, more active sites, high stability, and easy recoverability.[144]

For instance, Leeladee et al. developed a nanocomposite using 5,10,15,20-tetrakis(4-phenyl)Zn(II)porphyrin linked to GO by π-π stacking interaction (Scheme 8).[145] This synthesized nanocomposite oxidized benzyl alcohol with 82% yield of benzaldehyde under white LED light over 24 hours. However, the catalyst's reusability was limited, with a noticeable decrease in yield after the second cycle. To address this challenge, the researcher synthesized a covalently linked GO composite with Pd(II) porphyrin using 3-chloropropyl)trimethoxysilane.[146] This

composite was effective in Suzuki-Miyaura and Mizoroki-Heck coupling reactions, achieving 99% yield for the biaryl product and 95% yield of trans-stilbene, respectively (Scheme 9). The result demonstrated high catalytic activity and stability over five consecutive cycles without losing efficiency. Numerous studies have been reported on porphyrin/Pc@GO-based nanocomposites as catalysts for various reactions, including oxidation, reduction, cycloaddition, coupling, hydrogenation, and rearrangement reactions, which are tabulated in Table 6.

Scheme 8 Noncovalently linked GO/Zn(II)porphyrin nanocomposite employed in the oxidation of alcohol

Scheme 9 Covalently linked GO/Pd(II)porphyrin nanocomposite in the coupling reactions

Table 6 Porphyrin and phthalocyanine@GO-based nanocomposites utilized as catalysts in the organic transformations

Entry	Catalyst	Reactant	Product (Yield)	Reaction conditions	Reaction Type	References
1	GO–CuTAPP	phenylacetylene, morpholine, benzaldehyde	propargylamine (99 %)	DCE, 40 ℃, 30 min.	coupling	[147]

2	GO/NiTAPP	iodobenzene, phenylboronic acid	biaryl (95 %)	K_3PO_4, dioxane, 80 ℃, 1 h	Suzuki–Miyaura cross-coupling	[148]
3	GO-CoTAPP	benzaldoxime	benzamide (90 %)	toluene, 80 ℃, 2 h	Beckmann rearrangement	[144]
4	Mn(THPP)OAc@GO	cyclooctene	epoxide (78 %)	ImH, IBA, 45 ℃, 2 h	oxidation	[149]
5	GO-ZrTAPP	ethyl acetoacetate, 4-chlorobenzaldehyde, and urea	3,4-dihydropyrimidin-2(1H)-ones (92 %)	70 ℃, 40 min.	Biginelli reaction	[150]
6	GO-[Mn(TPyP)tart]	*cis*-stilbene	epoxide (100 %)	IBA, O_2, CH_3CN, 60 ℃, 2 h	oxidation	[151]
7	Mn(TAPP)Cl@GO	olefins	epoxide (95-52 %)	$NaIO_4$, CH_3CN/H_2O_2, ImH, RT, 2.5-3.5 h	oxidation	[152]
8	Mn(THPP)OAc@GO	thiolane	sulfoxides (100 %)	UHP, ethanol, RT, 35 min.	oxidation	[153]
9	Ru-PP/RGO	levulinic acid	γ-valerolactone (71 %)	CH_3OH, 100 ℃, 10 h	hydrogenation	[154]
10	GO-Sn-Porph	4- nitrophenol	4-aminophenol (99 %)	$NaBH_4$, 60 min.	reduction	[155]
11	NH_2SA-NiPor	4- nitrophenol	4-aminophenol (99 %)	$NaBH_4$, 60 min.	reduction	[156]
12	GO-[Mn(T2PyP)(tart)](tart)	*trans*-stilbene	epoxide (100 %)	visible light (40 W), ImH, DCM, O_2, ^iPrCHO, RT, 30 min.	oxidation	[157]
13	GO-CPTMS@Pd-TKHPP	iodobenzene, phenylboronic acid	biaryl (99 %)	K_2CO_3, EtOH/H_2O, 80 ℃, 5 min.	Suzuki-Miyaura coupling	[146]
		Iodobenzene, styrene	*trans*-stilbene (95 %)	K_2CO_3, DMF, 120 ℃, 20 min.	Mizoroki-Heck coupling	
14	GO–CuTAPP	azide, terminal alkyne	1,2,3-triazole (95 %)	H_2O/EtOH, 60 ℃, 15 min.	cycloaddition	[158]
15	GS/CuTHPP	CO_2	C_2H_4 (23 mmol g^{-1} h^{-1})	DCE, 100 mW cm^2, 40 ℃, 6 h	photoreduction	[159]
16	CoTSPP@N, P: GQDs/G	benzyl alcohol	benzaldehyde (92 %)	six 22 W lamps (32, 400 LUX), air (1 atm), water, RT, 10 h	photooxidation	[160]
17	CoTPP-NH_2@GO	epoxide, CO_2	cyclic carbonate (99-16 %)	CO_2 (1.8 MPa), 0.1mol% TBAI, 120 ℃, 12 h	cycloaddition	[161]
18	GO-Co-TAPP	CO_2	formic acid (96 µmol)	NADH, methyl viologen, 450 W xenon lamp, 2 h	photoreduction	[162]
19	Fe_3O_4.GO.Im@MnPor	cyclooctene	epoxide (96 %)	alkene:UHP:HOAc (1:100:200:300), DCM, RT, 1-1.5 h	oxidation	[163]
20	GO-TPP	alcohol	aldehyde/ketone (89-26 %)	white cold LED, 24 h	photo-oxidation	[164]
21	GO-FePc	alcohol	Ketone (97 %)	K_2CO_3, H_2O, O_2 (1 atm), 60 ℃, 3 h	oxidation	[165]
22	GO-CuPcS	CO_2, methanol	dimethyl carbonate (13 %)	CO_2 (25 bar), 110 ℃, 2.5 h	cycloaddition	[166]

TAPP: 5,10,15,20-tetrakis(aminophenyl)porphyrin; DCE: dichloroethane; THPP: 5,10,15,20-Tetrakis(4-hydroxyphenyl)porphyrin; ImH: Imidazole; IBA: isobutyraldehyde, TMPyP:5,10,15,20-tetrakis(1-methyl-4-pyridinio)porphyrin tetra(*p*-toluenesulfonate); T2PyP: *meso*-tetra(2-pyridyl)porphyrin; TPyP: Tetra pyridyl porphyrin; UHP: urea hydrogen peroxide; TPP-NH_2: 5-(4-Aminophenyl)-10,15,20-triphenyl porphyrin; TCPP: Meso-tetra-(4-carboxyphenyl)porphyrin

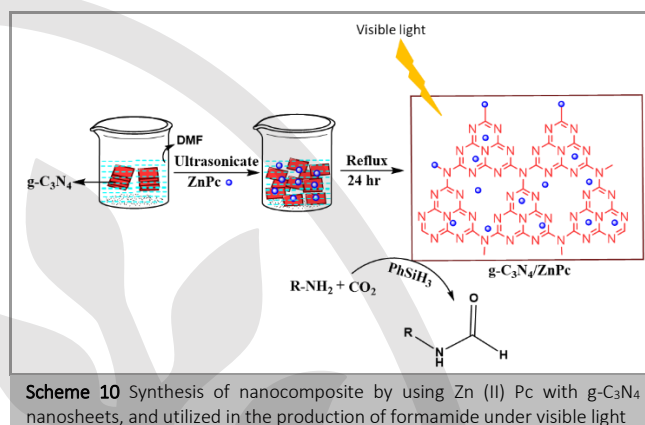### 2.3.3 Porphyrin and phthalocyanine nanocomposites with graphitic carbon nitrite

Graphitic carbon nitride (g-C₃N₄), is a polymeric compound of nitrogen and carbon atoms interconnected to form a layered structure. This material is notable for being a metal-free semiconductor with several advantageous properties, including non-toxicity, affordability, and excellent thermal and chemical stability.[167] It can be synthesized easily through the pyrolysis of readily available materials such as urea, thiourea, and melamine.[168] The bulk g-C₃N₄ has a limited surface area and poor light absorption, which hampers its photocatalytic efficiency. The synthesis of nanosheets from g-C₃N₄ significantly improves these characteristics.[169] These nanosheets of g-C₃N₄ possess a larger surface area and more active catalytic sites. However, they still face low-charge separation challenges, which restricts their practical applications.[169] To improve the photocatalytic activity of g-C₃N₄, researchers have explored its combination with other photoactive materials, such as porphyrin or phthalocyanine (Pc). The resulting hybrid nanomaterials, porphyrin/Pc@g-C₃N₄, demonstrate high photocatalytic efficiency under visible light.[170] This improvement is attributed to a reduction in the band gap and enhanced charge separation. When exposed to visible light, the

electrons in porphyrin/Pc become excited, transitioning from the highest occupied molecular orbital (HOMO) to the lowest unoccupied molecular orbital (LUMO).[171] Concurrently, electrons in g-C_3N_4 move from the valence band to the conduction band. The electron in the LUMO then transfers to the conduction band, while a hole moves from the valence band to the HOMO. This process indicates that the hybrid nanocomposite exhibits strong oxidation capabilities in the valence band and significant reducing abilities in the conduction band, facilitating reduction and oxidation reactions.[171] Many scientists also synthesized the nanocomposite of porphyrin/Pc@g-C_3N_4 and used it in different organic reactions under visible light (Table 7).

In a recent study, Jain et al. synthesized a ZPCN-5 nanocomposite by combining 5 wt% Zn(II)Pc with g-C_3N_4 nanosheets by noncovalent interactions.[172] This nanocomposite was utilized for the formation of formamide from amine and CO_2 in visible light (Scheme 10). The individual components, Zn(II)Pc and nano g-C_3N_4, exhibited 9% and 22% yields of formamide, respectively. However, the ZPCN-5 nanocomposite

demonstrated a remarkable enhancement in activity, achieving a 95% yield of formamide. This significant improvement highlighted the synergistic effect, which provides a larger surface area, reduces the band gap, and enhances charge separation, ultimately boosting photocatalytic activity.

Scheme 10 Synthesis of nanocomposite by using Zn (II) Pc with g-C_3N_4 nanosheets, and utilized in the production of formamide under visible light

Table 7 Reported porphyrin and phthalocyanine@g-C_3N_4-based nanocomposites used in the organic reactions

Entry	Catalyst	Reactant	Product (Yield)	Reaction conditions	Reaction Type	Reference
1	CoTPP/g-C_3N_4	CO_2	formic acid (154 μmol)	electrochemical	Photoreduction	[173]
2	ZnPp-g-C_3N_4-TE	5-hydroxymethyl-2-furfural	2,5-furandicarboxyaldehyde (38 %)	natural solar light, pH 7, 4 h	photo-oxidation	[170]
3	CoPc/g-C_3N_4	alcohol	aldehyde, and ketone (30-7 %)	O_2, CH_3CN, 30 ℃, UV-visible light, 6 h	photo-oxidation	[169]
4	CoPc/Py@g-C_3N_4	furoin, 1,2-phenylenediamines	quinoxalines (93 %)	visible light, KOH, CH_3OH, RT, 4 h	oxidative cyclization	[174]
5	ZnTcPc@g-C_3N_4	thiophene	sulfone (84 %)	visible light, molecular oxygen, 90 min.	desulfurization	[175]
6	g-C_3N_4/CoPc-COOH	CO_2	methanol (646 μmol)	LED light (20 W), 24 h	photoreduction	[171]
7	ZnPc/g-C_3N_4	amine, CO_2	formamide (95-24 %)	LED light (20 W), $PhSiH_3$, DMF, RT, 24 h	N-formylation	[172]
8	NiPc–FePc/BCN	benzyl alcohol	benzyl aldehyde (38 % with >99 % selectivity)	visible light, O_2	photo-oxidation	[176]
9	CoPc/NG/g-C_3N_4	benzyl alcohol	benzyl aldehyde (27 % with >99 % selectivity)	visible light, O_2	photo-oxidation	[177]

TBrPP: tetra(4-bromophenyl) porphyrin; CMP: g-C_3N_4 mesoporous polymer; TPP: meso-tetraphenylporphyrin; Pp: meso-tetra aryl substituted porphyrins; TE: thermo-exfoliated; TEA: triethylamine; DMA: N, N-dimethylacetamide; $PhSiH_3$: phenyl silane; BCN: boron doped g-C_3N_4; NG: nitrogen doped graphene

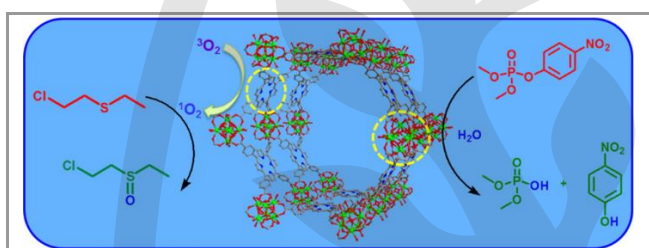## 2.4 Porphyrin and phthalocyanine-based nano-organic framework

Organic frameworks consist of repeating interconnected monomer units to form a framework-like structure with regular pores.[15] It exhibits unique properties such as high surface area, versatile framework, high porosity with uniform pores, and excellent stability.[15] These remarkable properties have garnered considerable attention from researchers around the world. Among the various porous materials, metal-organic frameworks (MOFs) and covalent organic frameworks (COFs) have garnered particular attention because of their high stability and catalytic activity.[178] The choice of organic linker influences the catalytic performance of these frameworks. Porphyrin, due to its high thermal stability and semiconducting properties, has been utilized in forming MOFs and COFs.[179]

Porphyrin-containing MOFs and COFs exhibit exceptional characteristics, including visible light absorption, excellent thermal stability, many active sites, and superior electron transfer properties, which enhance their photophysical and photochemical properties.[178,180] Additionally, the nanostructure of these materials plays a crucial role in their catalytic activity. Nanosized porphyrin-based MOFs and COFs demonstrate superior catalytic performance compared to their bulk counterparts, attributed to their increased surface area, more active site, and enhanced selectivity.[181]

For example, Farha et al. synthesized PCN-222/MOF-545 using $ZrOCl_2.8H_2O$, benzoic acid, and tetrakis(4-carboxyphenyl) porphyrin (TCPP).[182] This MOF was employed for the oxidation and hydrolysis of chemical warfare agents such as dimethyl 4-nitrophenyl phosphate (DMNP), and 2-chloroethyl ethyl sulfide
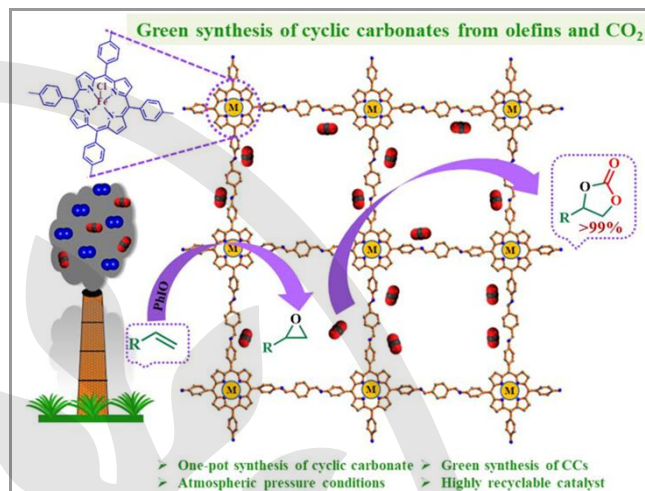
(CEES) under blue LED light in the presence of N-ethyl morpholine at room temperature (Scheme 11). The hydrolysis of DMNP resulted in the formation of nitrophenol and dimethyl phosphate with a half-life of 8 minutes. Meanwhile, CEES was oxidized to produce 2-chloroethyl ethyl sulfoxide and 2-aceto ethyl ethyl sulfoxide with a half-life of 12 minutes.

In another study, Nagaraja et al. synthesized nanosized Fe(III)P@COF using 5,10,15,20-tetrakis(4-aminobiphenyl)Fe(III)porphyrin and 1,4-benzenedicarboxaldehyde.[183] This COF was utilized to oxidize alkene in the presence of oxidant iodosyl benzene (PhIO), leading to epoxide formation. These synthesized epoxides were then used as a reactant in a cycloaddition reaction with CO_2 at 1 atm pressure, using TBAB as a co-catalyst to produce cyclic carbonates (Scheme 12). The catalyst demonstrated excellent stability, maintaining its efficiency over eight cycles. Other reported nanosized MOFs, and COFs with their catalytic activities have been summarized in Table 8.

detoxification of chemical warfare agent by hydrolysis and oxidation process under blue light, (Reproduced by the permission of reference[182], Copyright 2015 American Chemical Society)

Scheme 12 Iron-porphyrin-based nanosized Fe(III)P@COF used in the formation of epoxide from an alkene, and cyclic carbonate from an epoxide, (Reproduce by the permission of reference[183]. Copyright 2023 American Chemical Society)

Scheme 11 Free-base nanosized PCN-222/MOF-545 used in the

Table 8 Porphyrin-based nanosized MOFs and COFs employed in the organic reactions

Entry	Catalyst	Reactant	Product (yield)	Reaction Conditions	Reaction type	References
1	Ln(H$_9$ TPPA)(H$_2$O)$_x$]Cl$_2$·yH$_2$O MOF (x+y=7)	thioanisole	benzenesulfonic acid (80 %)	H$_2$O$_2$, CH$_3$CN, 50 ℃, 24 h	oxidation	[184]
2	Zn$_3$(TCPP)(bpy)$_{1.5}$(DMF)$_3$(H$_2$O)$_4$ MOF	oxathiolanes	ketones (conversion 100-97%)	Xe lamp (300 W), O$_2$ (1 atm), CH$_3$CN, 90-110 min.	deprotection	[185]
3	PCN-222/MOF-54	CEES	2-chloroethyl ethyl sulfoxide + 2-aceto ethyl ethyl sulfoxide	N-ethylmor-pholine, MeOH, O$_2$, H$_2$O, blue LED light	oxidation (t$_{1/2}$=12 min.)	[182]
		DMNP	nitrophenol + dimethyl phosphate		hydrolysis (t$_{1/2}$=8 min.)	
4	PCN-222	CEES	2-chloroethyl ethyl sulfoxide (TOF$_{t/2}$= 41.68 min^{-1})	hv, O$_2$, 120 min.	mustard photooxidation (t$_{1/2}$=12.6 min.)	[186]
		DMNP	phosphate (TOF$_{t/2}$= 15.66 min^{-1})	blue light, pH 10, H$_2$O, 150 min.	soman photohydrolysis (t$_{1/2}$=8 min.)	
5	HZ@TCPP-Fe/Cu	aromatic hydrazides	aromatic azobenzenes (90-18 %)	THF, RT, 4 h	oxidative dehydrogenation	[187]
6	PCN-222(Fe)	thymol	thymoquinone (94 %)	PMS, CH$_3$OH/H$_2$O, RT, 2 h	oxidation	[188]
7	Ir-PMOF1(Hf)	benzoic acid, ethyl diazoacetate	2-ethoxy-2-oxoethyl benzoate (80 %)	DCM, 9 min.	insertion	[189]
8	Ag@TAPP-COF	4-nitrophenol	4-aminophenol (>99 %)	200 sec.	reduction	[190]

9	Fe(III)@P-COF	olefins, CO_2	cyclic carbonates (99-40 %)	CO_2 (0.1 MPa), PhIO, TBAB, DCM, 80 ℃, 24 h	cycloaddition	[183]
		olefins	epoxide (99-38 %)	PhIO, DCM, 40 ℃, 18 h	epoxidation	
10	2,3-DhaTph	styrene oxide, CO_2	cyclic carbonates (94 %)	CO_2 (1 atm), TBAI, 110 °C, 12 h	cycloaddition	[191]
		aziridines, CO_2	oxazolidinones (96-39 %)	CO_2 (2 MPa), TBAI, 50 °C, 3-15 h		
11	Co-CoTCPP MOF	indane	indanone (selectivity-92 %)	O_2, 140 ℃, 22 h	aerobic Oxidation	[192]
12	Ag/TPP-CTF	propargyl alcohols, CO_2	α-alkylidene cyclic carbonates (96-77 %)	CO_2 (1 bar), RT, 12-48 h	cycloaddition	[193]

TPPA: 5,10,15,20-tetrakis(p-phenylphosphonic acid)porphyrin; CEES:2-chloroethyl ethyl sulfide, DMNP: dimethyl 4-nitrophenylphosphate; PCN-222/MOF-54: tetrakis(4-carboxyphenyl)porphyrin ($TCPP^{4-}$) and 8-connected Zr_6 cluster; PCN-222: zirconium–porphyrin based nano-crystalline MOF; HZ: hollow ZIF; PMS:peroxymonosulfate; Ir-PMOF1(Hf): $[(Hf_6(\mu_3-O)_8(OH)_2(H_2O)_{10})_2(Ir(TCPP)Cl)_3]\cdot solvents$; Fe(III)@P-COF: Fe-TAPP based COF; 2,3-Dha- 2,3-dihydroxyterephthalaldehyde, Tph- 5,10,15,20-tetrakis(4-aminophenyl)-21H,23H-porphine

3. Conclusion and Future Prospects

This review emphasizes the catalytic significance of porphyrin and phthalocyanine-based nanocomposites in modern chemistry. These nanocomposites demonstrate remarkable catalytic activity across various organic reactions, including oxidation, coupling, cycloaddition, reduction, hydrogenation, dechlorination, hydrolysis, rearrangement, and condensation reactions. Their ability to facilitate the synthesis of valuable products while utilizing waste materials is particularly beneficial for the industrial and pharmaceutical sectors. One of the key advantages of these nanocomposites is their capacity to function as a single catalyst in complex reactions that typically require multiple catalysts. This capability streamlines the reaction process and significantly enhances the overall reaction rate, making them highly effective in various applications. The modifications of porphyrin and phthalocyanines with different nanostructures through covalent and non-covalent interactions provide versatile catalysts that exhibit superior activities in varied organic transformations under mild conditions. However, deterioration of the catalysts, leading to poor reusability, is observed in some cases when nanomaterials are attached non-covalently with porphyrins and phthalocyanines. Additionally, the low yield associated with synthesizing porphyrin and phthalocyanine is another challenge, which may limit their broader applications. However, the ease of recovery and reusability of these nanocomposites have garnered considerable interest from researchers as they address sustainability concerns in chemical processes.

Beyond their catalytic applications, porphyrin and phthalocyanine-based nanocomposites have significant potential for advancing sensing technologies in environmental monitoring, food safety, and medical diagnostics. These nanocomposites are expected to enhance early disease detection, real-time health monitoring, and personalized healthcare solutions. In environmental applications, they provide high sensitivity for detecting toxic gases and pollutants, which is essential for effective pollution management and sustainable development. Their application in food safety includes monitoring freshness, detecting microbial contamination, and identifying toxic residues, with promising possibilities for integration into smart packaging systems. Additionally, their versatility also extends to clinical therapies, revolutionizing theragnostic platforms by merging precise disease detection with targeted treatment methods such as photodynamic therapy. The catalytic prospects of porphyrin and phthalocyanine-based nanostructures will lead to the development of industrial methods for synthesizing pharmaceuticals, agriculture chemicals, dyes, and other commercially important scaffolds.

Conflict of Interest

The author declares no conflict of interest.

References

(1) Poonam; Kumari, P.; Ahmad, S.; Chauhan, S. M. S. *Tetrahedron Lett.* **2011**, 52, 7083.

(2) Poonam; Kumari, P.; Grishina, M.; Potemkin, V.; Verma, A.; Rathi, B. *New J. Chem.* **2019**, 43, 5228.

(3) Poonam; Kumari, P.; Nagpal, R.; Chauhan, S. M. S. *New J. Chem.* **2011**, 35, 2639.

(4) Chauhan, S. M. S.; Kumari, P. *Tetrahedron Lett.* **2007**, 48, 5035.

(5) Kumari, P.; Nagpal, R.; Chauhan, P.; Yatindranath, V.; Chauhan, S. M. S. *J. Chem. Sci.* **2015**, 127, 13.

(6) Kumari, P.; Poonam; Chauhan, S. M. S. *Chem. Comm.* **2009**, 42, 6397.

(7) de Araujo Tôrres, M. G.; da Silva, V. S.; Idemori, Y. M.; DeFreitas-Silva, G. *Arabian J. Chem.* **2020**, 13, 1563.

(8) Cabral, B. N.; Milani, J. L. S.; Meireles, A. M.; Martins, D. C. da S.; Ribeiro, S. L. da S.; Rebouças, J. S.; Donnici, C. L.; das Chagas, R. P. *New J. Chem.* **2021**, 45, 1934

(9) Tripathi, D.; Yadav, I.; Negi, H.; Singh, R. K.; Srivastava, V. C.; Sankar, M. *J. Porphyrins Phthalocyanines* **2021**, 25, 24.

(10) Ishikawa, Y.; Kameyama, T.; Torimoto, T.; Maeda, H.; Segi, M.; Furuyama, T. *Chem. Comm*. **2021**, 57, 13594.

(11) Yüceel, Ç.; Şahin, Z.; Işci, Ü. *J. Porphyrins Phthalocyanines* **2022**, 26, 452.

(12) Gimadieva, A. R.; Khazimullina, Y. Z.; Abdrakhmanov, I. B.; Mustafi, A. G. *Russ. Chem. Bull.* **2023**, 72, 2372-2376.

(13) Bhaumik, J.; Gogia, G.; Kirar, S.; Vijay, L.; Thakur, N. S.; Banerjee, U. C.; Laha, J. K. *New J. Chem.* **2016**, 40, 724.

(14) Sannegowda, K.; Shambhulinga, A.; Manjunatha, N.; Imadadulla, M.; Hojamberdiev, M. *Dyes Pigm.* **2015**, 120, 155.

(15) Zhang, Y.; Jin, X.; Ma, X.; Wang, Y. *Anal. Methods* **2021**, 13, 8.

(16) Altammar, K. A. *Front. Microbiol.* **2023**, 14, 1155622.

(17) Yan, J.; Liu, G.; Li, N.; Zhang, N.; Liu, X. *Eur. J. Inorg. Chem.* **2019**, 2019, 2806.

(18) Narayan, N.; Meiyazhagan, A.; Vajtai, R. *Materials* **2019**, 12, 3602.

(19) Librando, I. L.; Mahmoud, A. G.; Carabineiro, S. A. C.; Guedes da Silva, M. F. C.; Maldonado-Hódar, F. J.; Geraldes, C. F. G. C.; Pombeiro, A. J. L. *Catalysts* **2021**, 12, 45.

(20) Yang, Y.; Li, Y.; Lu, Y.; Chen, Z.; Luo, R. *ACS Catal.* **2024**, 14, 10344.

(21) Chauke, V. P.; Antunes, E.; Chidawanyika, W.; Nyokong, T. *J. Mol. Catal. A Chem.* **2011**, 335, 121.

(22) Ding, Z. D.; Wang, Y. X.; Xi, S. F.; Li, Y.; Li, Z.; Ren, X.; Gu, Z. G *Chem.-Eur. J.* **2016**, 22, 17029.

(23) Limosani, F.; Remita, H.; Tagliatesta, P.; Bauer, E. M.; Leoni, A.; Carbone, M. *Materials* **2022**, 15, 1207.

(24) Chen, J.; Zhang, J.; Zhu, D.; Li, T. *Gold Bull*. **2019**, 52, 19.

(25) Zou, Z.; Jiang, Y.; Song, K. *Catal. Letters* **2020**, 150, 1277.

(26) Zhu, W.; Wang, X.; Li, T.; Shen, R.; Hao, S.-J.; Li, Y.; Wang, Q.; Li, Z.; Gu, Z.-G. *Polym. Chem.* **2018**, 9, 1430.

(27) Kumar, S.; Alka; Tarun; Saxena, J.; Bansal, C.; Kumari, P. *Appl. Nanosci.* **2020**, 10, 1555.

(28) Kumari, P.; Kumar, S.; Gupta, S.; Mishra, A.; Kumar, A. *ChemistrySelect* **2018**, 3, 2135.

(29) Kumari, P.; Parashara, H. *Mater. Today: Proc.* **2018**, 5, 15463-15470.

(30) Alka; Kumar, S.; Kumari, P. *Int. J. Enviorn. Sci. Technol.* **2023**, 20, 4467-4482.

(31) Kumari, P.; Alka; Kumar, S.; Nisa, K.; Kumar Sharma, D. *J. Environ. Chem. Eng.* **2019**, 7, 103130.

(32) Kumari, P.; Gautam, R.; Yadav, H.; Kushwaha, V.; Mishra, A.; Gupta, S.; Arora, V. *Catal. Letters* **2016**, 146, 2149.

(33) Zeleňáková, A.; Zeleňák, V.; Beňová, E.; Kočíková, B.; Király, N.; Hrubovčák, P.; Szűcsová, J.; Nagy; Klementová, M.; Mačák, J.; Závišová, V.; Bednarčík, J.; Kupčík, J.; Jacková, A.; Volavka, D.; Košuth, J.; Vilček *Sci. Rep.* **2024**, 14, 14427.

(34) Neamtu, M.; Nadejde, C.; Brinza, L.; Dragos, O.; Gherghel, D.; Paul, A. *Sci. Rep.* **2020**, 10, 5276.

(35) Bagherzadeh, M.; Hosseini, M.; Mortazavi-Manesh, A. *Inorg. Chem. Commun.* **2019**, 107, 107495.

(36) Mak, C. A.; Pericas, M. A.; Fagadar-Cosma, E. *Catal. Today* **2018**, 306, 268.

(37) Dias, L. D.; Carrilho, R. M. B.; Henriques, C. A.; Piccirillo, G.; Fernandes, A.; Rossi, L. M.; Filipa Ribeiro, M.; Calvete, M. J. F.; Pereira, M. M. *J. Porphyrins Phthalocyanines* **2018**, 22, 331.

(38) Heidari-Golafzani, M.; Rabbani, M.; Rahimi, R.; Azad, A. *RSC Adv.* **2015**, 5, 99640.

(39) Dashteh, M.; Baghery, S.; Zolfigol, M. A.; Khazaei, A.; Khajevand, M. *ChemistrySelect* **2022**, 7, e202202300.

(40) Rayati, S.; Nejabat, F.; Panjiali, F. *Catal. Commun.* **2019**, 122, 52.

(41) Bai, D.; Wang, Q.; Song, Y.; Li, B.; Jing, H. *Catal. Commun.* **2011**, 12, 684.

(42) Ucoski, G. M.; Pinto, V. H. A.; DeFreitas-Silva, G.; Rebouças, J. S.; Marcos da Silva, R.; Mazzaro, I.; Nunes, F. S.; Nakagaki, S. *Microporous and Mesoporous Mater.* **2018**, 265, 84.

(43) Dias, L. D.; Carrilho, R. M. B.; Henriques, C. A.; Piccirillo, G.; Fernandes, A.; Rossi, L. M.; Filipa Ribeiro, M.; Calvete, M. J. F.; Pereira, M. M. *J. Porphyrins Phthalocyanines* **2018**, 22, 331.

(44) Shokoohi, S.; Rayati, S. *J. Ira. Chem. Soc.* **2023**, 20, 1271.

(45) Shokoohi, S.; Rayati, S. *J. Porphyrins Phthalocyanines* **2022**, 26, 8.

(46) Rayati, S.; Moradi, D.; Nejabat, F. *New J. Chem.* **2020**, 44, 19385.

(47) Dias, L. D.; De Carvalho, A. L. M. B.; Pinto, S. M. A.; Aquino, G. L. B.; Calvete, M. J. F.; Rossi, L. M.; Marques, M. P. M.; Pereira, M. M. *Molecules* **2019**, 24, 52.

(48) Dan-Hua, S.; Lin-Tao, J.; Zhi-Gang, L.; Wen-Bin, S.; Can-Cheng, G. *J. Mol. Catal. A Chem.* **2013**, 379, 15.

(49) Bagherzadeh, M.; Mortazavi-Manesh, A. *J. Coord. Chem.* **2015**, 68, 2347.

(50) Naeimi, A.; Yoosefian, M. *J. Nanostruct.* **2019**, 9, 86.

(51) Rezaeifard, A.; Jafarpour, M.; Farshid, P.; Naeimi, A. *Eur. J. Inorg. Chem.* **2012**, 33, 5515-5524.

(52) Zolfigol, M. A.; Safaiee, M.; Bahrami-Nejad, N. *New J. Chem.* **2016**, 40, 5071.

(53) Safaiee, M.; Zolfigol, M. A.; Afsharnadery, F.; Baghery, S. *RSC Adv.* **2015**, 5, 102340.

(54) Naeimi, H.; Rahmatinejad, S. *J. Coord. Chem.* **2018**, 71, 4210.

(55) Singh, G.; Khatri, P. K.; Ganguly, S. K.; Jain, S. L. *RSC Adv.* **2014**, 4, 29124.

(56) Rezaeifard, A.; Jafarpour, M.; Naeimi, A.; Haddad, R. *Green Chem.* **2012**, 14, 3386.

(57) Ebadi, A.; Shojaei, S. *J. Nanostruct.* **2017**, 7, 57.

(58) La, D. D.; Rananaware, A.; Thi, H. P. N.; Jones, L.; Bhosale, S. V. *Adv. Nat. Sci.: Nanosci. and Nanotechnol.* **2017**, 8, 015009.

(59) Ahmed, M. A.; Abou-Gamra, Z. M.; Medien, H. A. A.; Hamza, M. A. *J. Photochem. Photobiol. B* **2017**, 176, 25.

(60) Askari, P.; Mohebbi, S. *New J. Chem.* **2018**, 42, 1715.

(61) Zhao, Z.; Fan, J.; Xie, M.; Wang, Z. *J. Clean. Prod.* **2009**, 17, 1025.

(62) Zhu, S.; Liu, P.; Hong, X. *ChemistrySelect* **2024**, 9, e202400596.

(63) Nikoloudakis, E.; Pati, P. B.; Charalambidis, G.; Budkina, D. S.; Diring, S.; Planchat, A.; Jacquemin, D.; Vauthey, E.; Coutsolelos, A. G.; Odobel, F. *ACS Catal.* **2021**, 11, 12075.

(64) Alamgholiloo, H.; Rostamnia, S.; Zhang, K.; Lee, T. H.; Lee, Y. S.; Varma, R. S.; Jang, H. W.; Shokouhimehr, M. *ACS Omega* **2020**, 5, 5182.

(65) Murphy, S.; Saurel, C.; Morrissey, A.; Tobin, J.; Oelgemöller, M.; Nolan, K. *Appl. Catal. B* **2012**, 119, 156-165.

(66) Li, K.; Lin, L.; Peng, T.; Guo, Y.; Li, R.; Zhang, *J. Chem. Commun.* **2015**, 51, 12443.

(67) Song, Y.; Li, J.; Wang, C. *J. Mater. Res.* **2018**, 33, 2612.

(68) Safaei, E.; Mohebbi, S. *J. Mater. Chem. A Mater.* **2016**, 4, 3933.

(69) Ghobadifard, M.; Safaei, E.; Radovanovic, P. V.; Mohebbi, S. *New J. Chem.* **2021**, 45, 8032.

(70) Xiao, T.; Chen, Y.; Liang, Y. *J. Phys. Chem. C* **2022**, 126, 9742.

(71) Qiao, X.; Xiong, Z.; Zhang, Z.; Wang, R.; Qiu, S. *Appl. Surf. Sci.* **2023**, 608, *155182*.

(72) Abdulaeva, I. A.; Birin, K. P.; Chassagnon, R.; Bessmertnykh-Lemeune, A. *Catalysts* **2023**, 13, 402.

(73) Wang, Q.; Wu, W.; Chen, J.; Chu, G.; Ma, K.; Zou, H. *Colloids Surf. A* **2012**, 409, 118.

(74) Fan, J.; Zhao, Z.; Zhu, L.; Wang, Z. *Asian J. Chem.* **2014**, 26, 667.

(75) Kumar, P.; Chauhan, R. K.; Sain, B.; Jain, S. L. *Dalton Trans.* **2015**, 44, 4546.

(76) Li, L.; Wang, Y.; Ruan, Y.; Xu, T.; Wu, S.; Lu, W. *Appl. Surf. Sci.* **2024**, 672, 160771.

(77) Liu, S.; Zhao, Z.; Wang, Z. *Photochem. Photobiol. Sci.* **2007**, 6, 695.

(78) Zhao, Z.; Fan, J.; Liu, S.; Wang, Z. *Chem. Eng. J.* **2009**, 151, 134.

(79) Bansal, A.; Kumar, A.; Kumar, P.; Bojja, S.; Chatterjee, A. K.; Ray, S. S.; Jain, S. L. *RSC Adv.* **2015**, 5, 21189.

(80) Hughes, K. J.; Iyer, K. A.; Bird, R. E.; Ivanov, J.; Banerjee, S.; Georges, G.; Zhou, Q. A. *ACS Appl. Nano Mater.* **2024**, 7, 18695.

(81) Thole, D.; Modibane, K. D.; Mhlaba, R.; Balogun, S. A.; Malgas-Enus, R.; Botha, E.; Musyoka, N. M.; van Sittert, C. G. C. E. *Results Chem.* **2024**, 7, 101496.

(82) Saifuddin, N.; Raziah, A. Z.; Junizah, A. R. *J. Chem.* **2013**, 2013, 676815.

(83) Zhang, T.; Ge, Y.; Wang, X.; Chen, J.; Huang, X.; Liao, Y. *ACS Omega* **2017**, 2, 3228.

(84) Jayakumar, S.; Li, H.; Chen, J.; Yang, Q. *ACS Appl. Mater. Interfaces* **2018**, 10, 2546.

(85) Nazeri, M. T.; Javanbakht, S.; Ramezani, M.; Shaabani, A. *J. Taiwan Inst. Chem. Eng.* **2022**, 136, 104428.

(86) Kargar, H.; Moghadam, M.; Mirkhani, V.; Tangestaninejad, S.; Mohammadpoor-Baltork, I.; Rezaei, S. *Transition Met. Chem.* **2013**, 38(1), 1-5.

(87) Rayati, S.; Jafarzadeh, P.; Zakavi, S. *Inorg. Chem. Commun.* **2013**, 29, 40.

(88) Rayati, S.; Nejabat, F. *New J. Chem.* **2017**, 41, 7987.

(89) Rezaeifard, A.; Jafarpour, M. *Catal. Sci. Technol.* **2014**, 4, 1960.

(90) Rayati, S.; Nejabat, F. *Comptes Rendus Chimie* **2017**, 20, 967.

(91) Lipińska, M. E.; Rebelo, S. L. H.; Freire, C. *J. Mater. Sci.* **2014**, 49, 1494.

(92) Moghadam, M.; Mohammadpoor-Baltork, I.; Tangestaninejad, S.; Mirkhani, V.; Kargar, H.; Zeini-Isfahani, N. *Polyhedron* **2009**, 28, 3816.

(93) Rayati, S.; Nejabat, F.; Radmanesh, P. *J. Coord. Chem.* **2021**, 74, 1336.

(94) Rayati, S.; Sheybanifard, Z *J. Porphyrins Phthalocyanines* **2015**, 19, 622.

(95) Rayati, S.; Bohloulbandi, E. *Comptes Rendus Chimie* **2014**, 17, 62.

(96) Abdinejad, M.; Dao, C.; Deng, B.; Dinic, F.; Voznyy, O.; Zhang, X. A.; Kraatz, H. B. *ACS Sustain. Chem. Eng.* **2020**, 8, 9549.

(97) Campisciano, V.; Valentino, L.; Morena, A.; Santiago-Portillo, A.; Saladino, N.; Gruttadauria, M.; Aprile, C.; Giacalone, F. *J. CO2 Util.* **2022**, 57, 101884.

(98) Rayati, S.; Malekmohammadi, S. *J. Exp. Nanosci.* **2016**, 11, 872.

(99) Rayati, S.; Sheybanifard, Z. *Comptes Rendus Chimie* **2016**, 19, 371.

(100) Araghi, M.; Bokaei, F. *Polyhedron* **2013**, 53, 15.

(101) Sharghi, H.; Beyzavi, M. H.; Safavi, A.; Doroodmand, M. M.; Khalifeh, R. *Adv. Synth. Catal.* **2009**, 351, 2391.

(102) Qiu, Y.; Yang, C.; Huo, J.; Liu, Z. *J. Mol. Catal. A Chem.* **2016**, 424, 276.

(103) Karimipour, G. *Int. J. Chem. Eng. Appl.* **2014**, 5, 194.

(104) Rayati, S.; Bohloulbandi, E.; Zakavi, S. *J. Coord. Chem.* **2016**, 69, 638.

(105) He, Q.; Li, H.; Hu, Z.; Lei, L.; Wang, D.; Li, T. T. *Angew. Chem., Int. Ed.* **2024**, 63, e202407090.

(106) Tchuiteng Kouatchou, J. A.; Farah, J.; Malloggi, F.; Gravel, E.; Doris, E. *ChemCatChem* **2024**, 16, e202400685.

(107) Bai, X.; Song, D.; Wei, J.; Wang, D.; Li, *J. Catal. Letters* **2022**, 152, 2227.

(108) Nejabat, F.; Rayati, S. *ChemistrySelect* **2022**, 7, e202104069.

(109) Valentino, L.; Campisciano, V.; Célis, C.; Lemaur, V.; Lazzaroni, R.; Gruttadauria, M.; Aprile, C.; Giacalone, F. *J. Catal.* **2023**, 428, 115143.

(110) Nejabat, F.; Rayati, S. *J. Ind. Eng. Chem.* **2019**, 69, 324.

(111) Rayati, S.; Pournaser, N.; Nejabat, F.; Nafarieh, *Inorg. Chem. Commun.* **2019**, 107, 107447.

(112) Rayati, S.; Zamanifard, A.; Nejabat, f.; Hoseini, S. *Mol. Catal.* **2021**, 516, 111950.

(113) Rayati, S.; Nafarieh, P. *Appl. Organomet. Chem.* **2019**, 33, 4789.

(114) Anjali, K.; Nishimura, S. *J. Catal.* **2023**, 428, 115182.

(115) Gharaati, S.; Kargar, H.; Falahati, A. M. *J. Iran. Chem. Soc.* **2017**, 14, 1169.

(116) Rayati, S.; Chegini, E. *Macroheterocycles* **2016**, 9, 151.

(117) Wan, Y.; Liang, Q.; Li, Z.; Xu, S.; Hu, X.; Liu, Q.; Lu, D. *J. Mol. Catal., A Chem.* **2015**, 402, 29.

(118) Wang, Z.; Sun, Z.; Li, Q.; Zhou, M.; Liang, Q.; Li, Z.; Sun, D. *Solid State Sci.* **2020**, 101, 106122.

(119) Wang, L.; Pan, D.; Zhou, M.; Liang, Q.; Li, Z. *Solid State Sci.* **2021**, 113, 106546.

(120) Li, Q.; Wang, Z.; Liang, Q.; Zhou, M.; Xu, S.; Li, Z.; Sun, D. *Fullerenes Nanotubes Carbon Nanostruct.* **2020**, 28, 799.

(121) Chen, B.; Zou, H.; Gong, L.; Zhang, H.; Li, N.; Pan, H.; Wang, K.; Yang, T.; Liu, Y.; Duan, L.; Liu, J.; Jiang *J. Appl. Catal. B* **2024**, 344, 123650.

(122) Wu, Y.; Jiang, Z.; Lu, X.; Liang, Y.; Wang, H. *Nature* **2019**, 575, 639.

(123) Chen, X.; Hu, X.; An, L.; Zhang, N.; Xia, D.; Zuo, X.; Wang, X. *Electrocatalysis* **2014**, 5, 68.

(124) Rooney, C. L.; Wu, Y.; Tao, Z.; Wang, H. *J. Am. Chem. Soc.* **2021**, 143, 19983.

(125) Li, Q.; Sun, Z.; Zhou, M.; Liang, Q.; Li, Z.; Xu, S. *J. Mater. Sci.: Mater. Electron.* **2019**, 30, 6277.

(126) Yang, Z. W.; Chen, J. M.; Qiu, L. Q.; Xie, W. J.; He, L. N. *Catal. Sci. Technol.* **2022**, 12, 5495.

(127) Choi, C.; Wang, X.; Kwon, S.; Hart, J. L.; Rooney, C. L.; Harmon, N. J.; Sam, Q. P.; Cha, J. J.; Goddard, W. A.; Elimelech, M.; Wang, H. *Nat. Nanotechnol.* **2023**, 18, 160.

(128) Ju, L.; Li, Z.; Xu, S.; Li, Q. *Fullerenes Nanotubes Carbon Nanostruct.* **2017**, 25, 335.

(129) Mohammad, E. J.; Kareem, M. M.; Atiyah, A. *J. Bull. Chem. Soc. Ethiop.* **2022**, 36, 197.

(130) Guo, T.; Wang, X.; Xing, X.; Fu, Z.; Ma, C.; Bedane, A. H.; Kong, L. *Environ. Sci. Pollut. Res. Int.* **2023**, 30, 122755.

(131) Chan, T.; Kong, C. J.; King, A. J.; Babbe, F.; Prabhakar, R. R.; Kubiak, C. P.; Ager, J. W. *ACS Appl. Energy Mater.* **2024**, 7, 3091.

(132) Zhang, F.; Zhang, Y.; Zhou, M.; Li, Z.; Xu, S. *Inorganica Chim. Acta* **2023**, 556, 121640.

(133) Zhu, Q.; Rooney, C. L.; Shema, H.; Zeng, C.; Panetier, J. A.; Gross, E.; Wang, H.; Baker, L. R. *Nat. Catal.* **2024**, 7, 987.

(134) Musgrave, C. B.; Li, Y.; Luo, Z.; Goddard, W. A. *Nano Energy* **2023**, 118, 108966.

(135) Cheon, S.; Zhu, S.; Gao, Y.; Li, J.; Harmon, N. J.; Zhang, W.; Francisco, J. S.; Zhu, C.; Wang, H. *J. Am. Chem. Soc.* **2024**, 156(36), 25151-25157.

(136) Rooney, C. L.; Lyons, M.; Wu, Y.; Hu, G.; Wang, M.; Choi, C.; Gao, Y.; Chang, C. W.; Brudvig, G. W.; Feng, Z.; Wang, H. *Angew. Chem., Int. Ed.* **2024**, 63, e202310623.

(137) Li, A. Z.; Yuan, B. J.; Xu, M.; Wang, Y.; Zhang, C.; Wang, X.; Wang, X.; Li, J.; Zheng, L.; Li, B. J.; Duan, H. *J. Am. Chem. Soc.* **2024**, 146, 5622.

(138) Zhu, Y.; Murali, S.; Cai, W.; Li, X.; Suk, J. W.; Potts, J. R.; Ruoff, R. S. *Adv. Mater.* **2010**, 22, 3906.

(139) Yu, W.; Sisi, L.; Haiyan, Y.; Jie, L. *RSC Adv.* **2020**, 10, 15328.

(140) Chen, D.; Feng, H.; Li. *J. Chem. Rev.* **2012**, 112, 6027.

(141) Nisa, K.; Singhal, A.; Kumari, P. *Curr. Org. Synth.* **2019**, 16, 154-159.

(142) Raveena; Alka; Gandhi, N.; Kumari, P. *ChemistrySelect* **2023**, 8(3), e202203431.

(143) Raveena; Singh, M. P.; Sengar, M.; Kumari, P. *ChemistrySelect* **2024,** 8(2), e202203272.

(144) Ghadamyari, Z.; Khojastehnezhad, A.; Seyedi, S. M.; Shiri, A. *ChemistrySelect* **2019**, 4, 10920-10927.

(145) Phuangburee, T.; Solonenko, D.; Plainpan, N.; Thamyongkit, P.; Zahn, D. R. T.; Unarunotai, S.; Tuntulani, T.; Leeladee, P. *New J. Chem.* **2020**, 44, 8264.

(146) Bahrami, K.; Kamrani, S. N. *Appl. Organomet. Chem.* **2018**, 32, e4104.

(147) Gou, F.; Liu, J.; Ye, N.; Jiang, X.; Qi, C. *J. CO2 Util.* **2021**, 48, 101534.

(148) Keyhaniyan, M.; Shiri, A.; Eshghi, H.; Khojastehnezhad, A. *New J. Chem.* **2018**, 42, 19433.

(149) Rayati, S.; Rezaie, S.; Nejabat, F. *Comptes Rendus Chimie* **2018**, 21, 696-703.

(150) Ghadamyari, Z.; Shiri, A.; Khojastehnezhad, A.; Seyedi, S. M. *Appl. Organomet. Chem.* **2019**, 33, e5091.

(151) Berijani, K.; Farokhi, A.; Hosseini-Monfared, H.; Janiak, C. *Tetrahedron* **2018**, 74, 2202-2210.

(152) Zarrinjahan, A.; Moghadam, M.; Mirkhani, V.; Tangestaninejad, S.; Mohammadpoor-Baltork, I. *J. Iran. Chem. Soc.* **2016**, 13, 1509-1516.

(153) Rayati, S.; Rezaie, S.; Nejabat, F. *J. Coord. Chem.* **2019**, 72, 1466-1479.

(154) Zhang, T.; Ge, Y.; Wang, X.; Chen, J.; Huang, X.; Liao, Y. *ACS Omega* **2017**, 2, 3228-3240.

(155) Yasmeen, R.; Singhaal, R.; Bajju, G. D.; Sheikh, H. N. *J. Chem. Sci.* **2022**, 134, 111.

(156) Ahmed, A.; Devi, G.; Kapahi, A.; Kundan, S.; Katoch, S.; Bajju, G. D. *J. Mater. Sci.: Mater. Electron.* **2019**, 30, 19738-19751.

(157) Ahadi, E.; Hosseini-Monfared, H.; Spieß, A.; Janiak, C. *Catal. Sci. Technol.* **2020**, 10, 3290-3302.

(158) Khojastehnezhad, A.; Bakavoli, M.; Javid, A.; Khakzad Siuki, M. M.; Shahidzadeh, M. *Res. Chem. Intermed.* **2019**, 45, 4473-4485.

(159) Piao, M.; Liu, N.; Wang, Y.; Feng, C. *Aust. J. Chem.* **2016**, 69, 27-32.

(160) Mahyari, M.; Nasrollah Gavgani, *J. Res. Chem. Intermed.* **2018**, 44, 3641-3657.

(161) Gou, F.; Liu, J.; Ye, N.; Jiang, X.; Qi, C. *J. CO2 Util.* **2021**, 48, 101534.

(162) Kumar, S.; Yadav, R. K.; Ram, K.; Aguiar, A.; Koh, J.; Sobral, A. J. F. N. *J. CO2 Util.* **2018**, 27, 107-114.

(163) Hajian, R.; Bahrami, E. *Catal. Lett.* **2022**, 152, 2445.

(164) Phuangburee, T.; Solonenko, D.; Plainpan, N.; Thamyongkit, P.; Zahn, D. R. T.; Unarunotai, S.; Tuntulani, T.; Leeladee, P. *New J. Chem.* **2020**, 44, 8264.

(165) Mahyari, M.; Shaabani, A. *Appl. Catal. A Gen.* **2014**, 469, 524.

(166) Kumar, S.; Kumar, P.; Jain, S. L. *J. Mater. Chem. A Mater.* **2014**, 2, 18861.

(167) Zou, W.; Liu, X. H.; Xue, C.; Zhou, X. T.; Yu, H. Y.; Fan, P.; Ji, H. B. *Appl. Catal. B* **2021**, 285, 119863.

(168) Ismael, M.; Wu, Y.; Taffa, D. H.; Bottke, P.; Wark, M. *New J. Chem.* **2019**, 43, 6909.

(169) Chu, X.; Qu, Y.; Zada, A.; Bai, L.; Li, Z.; Yang, F.; Zhao, L.; Zhang, G.; Sun, X.; Yang, Z. Di; Jing, L. *Adv. Sci.* **2020**, 7, 2001543.

(170) García-López, E. I.; Pomilla, F. R.; Bloise, E.; Lü, X. fei; Mele, G.; Palmisano, L.; Marcì, G. *Top. Catal.* **2021**, 64, 758.

(171) Kumar, A.; Prajapati, P. K.; Aathira, M. S.; Bansiwal, A.; Boukherroub, R.; Jain, S. L. *J. Colloid Interface Sci.* **2019**, 543, 201.

(172) Malik, A.; Prajapati, P. K.; Abraham, B. M.; Bhatt, S.; Basyach, P.; Jain, S. L. *Catal. Sci. Technol.* **2022**, 12 (8), 2688-2740.

(173) Liu, J.; Shi, H.; Shen, Q.; Guo, C.; Zhao, G. *Green Chem.* **2017**, 19, 5900.

(174) Jin, M.; Mohsen Sadeghzadeh, S.; Chen, *J. Energy Chem.* **2023**, 82, 638.

(175) Zhang, G.; Ren, J.; Zhao, W.; Tian, M.; Chen, W. *Res. Chem. Intermed.* **2018**, 44, 5547.

(176) Liu, H.; Chu, X.; Bai, L.; Yang, Z.; Jiao, Y.; Li, W.; Zhang, Y.; Jing, L. *J. Mater. Chem. A Mater.* **2022**, 10, 12062.

(177) Chu, X.; Liu, H.; Yu, H.; Bai, L.; Yang, F.; Zhao, L.; Zhao, Z.; Jiao, Y.; Li, W.; Zhang, G.; Jing, L. *Mater. Today Energy* **2022**, 25, 100963.

(178) Zhang, Y.; Lu, G.; Zhao, D.; Huang, X. *Mater. Chem. Front.* **2023**, 7, 4782.

(179) Tang, C.; Li, X.; Hu, Y.; Du, X.; Wang, S.; Chen, B.; Wang, S. *Molecules* **2024**, 29, 467.

(180) Jin, J. *New J. Chem.* **2020**, 44, 15362.

(181) Qin, Y.; Li, Z.; Duan, Y.; Guo, J.; Zhao, M.; Tang, Z. *Matter* **2022**, 5, 3260.

(182) Liu, Y.; Moon, S. Y.; Hupp, J. T.; Farha, O. K. *ACS Nano* **2015**, 9, 12358.

(183) Singh, G.; Prakash, K.; Nagaraja, C. M. *Inorg. Chem.* **2023**, 62, 13058.

(184) Pereira, C. F.; Figueira, F.; Mendes, R. F.; Rocha, J.; Hupp, J. T.; Farha, O. K.; Simoães, M. M. Q.; Tomé, J. P. C.; Paz, F. A. A. *Inorg. Chem.* **2018**, 57, 3855.

(185) Zhao, F. Y.; Li, W. J.; Guo, A.; Chang, L.; Li, Y.; Ruan, W. J. *RSC Adv.* **2016**, 6, 26199.

(186) Barton, H. F.; Jamir, J. D.; Davis, A. K.; Peterson, G. W.; Parsons, G. N. *Chem.-Eur. J.* **2021**, 27, 1465.

(187) Zhang, D.; Du, P.; Liu, J.; Zhang, R.; Zhang, Z.; Han, Z.; Chen, J.; Lu, X. *Small* **2020**, 16, 2004679.

(188) Günay Semerci, T.; Gönül; Gülmez, B.; Çimen Mutlu, Y. *ChemistrySelect* **2020**, 5, 14223.

(189) Wang, Y.; Cui, H.; Zhang, L.; Su, C. Y. *ChemCatChem* **2018**, 10, 3901.

(190) Zhu, Q.; Li, Y. L.; Yang, J.; Jia, X. M.; Luo, Y. H.; Zhang, D. E. *Solid State Sci.* **2024**, 147, 107398.

(191) Saptal, V.; Shinde, D. B.; Banerjee, R.; Bhanage, B. M. *Catal. Sci. Technol.* **2016**, 6, 6152.

(192) Uscategui-Linares, A.; Santiago-Portillo, A.; Navalón, S.; Dhakshinamoorthy, A.; Albero, J.; Parvulescu, V.; García, H. *Mol. Catal.* **2024**, 564, 114288.

(193) Yang, Y.; Li, Y.; Zhang, Z.; Chen, K.; Luo, R. *ACS Appl. Mater. Inter.* **2024**, 16, 411-424.

Biosketches

Raveena received her Bachelor's degree from Maharani's College, University of Rajasthan, Jaipur, and completed her master's degree at the University of Rajasthan, Jaipur. She is pursuing her PhD under the supervision of Dr. Pratibha Kumari, Deshbandhu College, University of Delhi. Her research interests include catalysis, materials science, and biomaterials science.

Dr Anju Bajaj received PhD under the supervision of Prof. SMS Chauhan from the Department of Chemistry at the University of Delhi. She is currently working as an Associate Professor at ARSD College, University of Delhi. Her research interest lies in Synthesis and mechanistic Organic Chemistry. She has published many research papers in national and international reputed journals.

Astha Tripathi completed her Bachelor's degree from SHUATS, Allahabad, before earning her M.Sc. in Medicinal Chemistry and Drug Designing from Guru Gobind Singh Indraprastha University, Delhi. She is currently pursuing her Ph.D. in Chemistry under the guidance of Dr. Pratibha Kumari at Deshbandhu College, University of Delhi. Astha's research interests encompass Material Science, Bio-organic Materials, and Analytical Chemistry, reflecting her commitment to advancing knowledge in these fields.

Dr Pratibha Kumari is currently working as an Associate Professor (Chemistry) at Deshbandhu College, University of Delhi, New Delhi, India. She received her BSc, MSc, MPhil, and PhD degrees from the University of Delhi, New Delhi, India. She worked on green energy production as a visiting Professor (INDO-US fellow) at San Diego State University, California, USA, in 2020. She received the prestigious INSA Visiting Scientists 2023-2024 award for her research in catalysis and electrocatalysis. Her research interests include catalysis, sensing, energy conversions, and bioorganic materials.